

Article

Earth as a time crystal: macroscopic nature of a quantum-scale phenomenon from transformative moderation of geomagnetic polarity, topography, and climate by precession resonance due to many-body entrainment

Mensur Omerbashich

Geophysics Online, Los Angeles, CA 90250, <https://orcid.org/0000-0003-1823-4721>
 Correspondence: omerbashich@geophysics.online, editor@geophysicsjournal.com

Abstract: Claims of paleodata periodicity are many and controversial, so that, for example, superimposing Phanerozoic (0–541 My) mass-extinction periods renders life on Earth impossible. This period hunt coincided with the modernization of geochronology, which now ties geological timescales to orbital frequencies. Such tuneup simplifies energy-band (variance-) stratification of information contents, enabling the separation of astronomical signals from harmonics, e.g., using variance-based spectral analysis. I thus show on diverse data (geomagnetic polarity, cratering, extinction episodes) as a proxy of planetary paleodynamics that many-body subharmonic entrainment induces a resonant response of the Earth to astronomical forcing so that the 2π -phase-shifted axial precession $p=26$ ky, and its $P_i=2\pi p/i$; $i=1, \dots, n$ harmonics, get resonantly responsible for virtually all paleodata periods. This resonantly quasiperiodic nature of strata is co-triggered by a $p'/4$ -lockstep to the $p'=41$ -ky obliquity (also 2π -phase-shifted, to $P'=3.5$ -My super-period). For verification, residuals analysis after suppressing $2\pi p$ (and thus P_i , too) in the current polarity-reversals GPTS-95 timescale's calibration extending to end-Campanian (0–83 My) successfully detected weak signals of Earth-Mars planetary resonances, reported previously from older epochs. The significant intrinsic residual signal is 26.5-My *Rampino period* — the carrier wave of crushing deflections co-responsible for transformative polarity reversals. While the $(2\pi p, P_i)$ resonant response of the Earth to orbital forcing is the long-sought energy transfer mechanism of the Milankovitch theory, fundamental system properties — 2π -phase-shift, $\frac{1}{4}$ lockstep to a forcer, and the discrete time translation symmetry (multiplied or halved periods) — previously thought confined to (quantum) time crystal, here appear macroscopic, rendering the concept of time crystal unremarkable. In turn, such a surprising cross-scale outcome has confirmed the main result: that of planetary precession being a cataclysmic geodynamic phenomenon as claimed in the past, e.g., as the mechanism for Earth expansion; then a time crystal in quantum dynamics could be due to particle entrainment, such as the collisions resulting in Feshbach resonances.

Keywords: macroscopic time crystals; measure-preserving dynamical systems; many-body entrainment; precession resonance; geomagnetic polarity reversals; topography-shaping events; Milankovitch theory; Earth expansion

1. Introduction

Any data used to monitor changes rely on a timescale to associate correctly times of changes with the respective values in a record of changes (called then a time-series). Geochronology develops methods to achieve the correct timing of such changes in geological time series.

Traditionally, one of the fundamental aims of geochronological studies has been drawing up a timescale that embraces the totality of geological events. Thus a timescale must provide as precise data as possible on the absolute age of the formations. The paleontological and lithological methods often allow stratigraphers to establish, for a studied sedimentary series, a very finely calibrated scale on which the numerous degrees are generally marked by characteristic fossils. Obviously, such scales cannot indicate the absolute ages: they remain relative scales. (IUGS, 1967)

Among various ways to construct a timescale for dating records of paleodata both accurately and precisely (including traditional methods: radiometric dating, biochronology, and magnetostratigraphy), the calibrating of paleodata using astrochronology has become the favored method in the 21st century. In astronomically tuned timescales, dates of samples dated with traditional techniques, particularly those with strata series missing, are purposely and usually at their ends re-matched to nearest astronomical cycles, most commonly of Earth's and planetary precessions. This tuneup makes very long (spanning millions of years, or My) astrochronologically dated records and their calibration points especially, excellent gauges for spectral analyses of paleodata in the quest for periodicity impressed by physical processes in broadest bands of energies within the Earth's vicinity. Calibration points of a geological timescale are the most accurately (traditionally) dated benchmarks that define that timescale.

Besides the above advantages of astronomical tuning, significant drawbacks became evident too, particularly those due to uncritical ways in which end-users approach the paleodata record analysis. Diversity studies are one such example. Thus despite a looming question of whether intensified diversity over the last 100 My is real or reflects sampling bias and other troubles, reports of such a varied diversity, and to that associated (allegedly) periodic mass extinctions from paleodata, have persisted for well over two centuries and have even picked pace in the 1980s (Smith, 2007). This hype then resulted in a hotly debated topic in which two sides have emerged — proponents of and opponents to the idea of periodic mass extinctions; see, for example, Bailer-Jones (2009). The seemingly eternal topic itself has coincided in time with the modernization of geological timescales, which became tied to natural astronomical cycles with the primary goal to enable a more realistic view of the Earth's system dynamics following the first confirmations of the Milankovitch (1941) theory of astronomically forced climate from deep drilling experiments, e.g., by Emiliani (1955).

Such astronomical calibration of paleodata time-series based on cyclostratigraphy, i.e., the identifying and counting cycles in strata, has been praised as an achievement of modern geology; see, e.g., Hinnov and Ogg (2007). However, others were critical for creating an analytical bias against research seeking to modify or replace the Milankovitch theory, e.g., Puetz et al. (2016). Also, there is criticism for contradicting biostratigraphy and inconsistencies due to lack of data in the stratigraphic record, particularly for data older than ~40 My, e.g., Tanner and Lucas (2014). Indeed, the field of applied astrochronology carries with itself fundamental computational problems like separating the astronomical signal from climatic and stratigraphic noise and understanding how the astronomical signal propagates through the climate system and into the stratigraphic record (Hinnov, 2013). In addition, determining rapid geomagnetic variations like reversals with adequate temporal precision is difficult since astronomical tuning nowadays is precise to better than 20 ky — a span still exceeding reversals short duration (Valet and Fournier, 2016). However, none of these potential problems identified in the past seems unsurmountable provided the right choices in data processing and analysis.

Earth's orbital cycles might be pacing the correlations and cyclicity seen in the geologic episodes. The occurrences of these cyclical episodes support the case for a largely periodic, coordinated, and intermittently catastrophic geologic record, which is quite different from the views held by most geologists. (Rampino et al., 2021)

2. Explanatory definitions

Various periodic celestial phenomena affect our planet noticeably every day. Earth's orbital *eccentricity* is one such phenomenon, albeit relatively mildest of them all. Gravitationally most powerful neighbors — Moon and Sun — cause *nutation*, *obliquity*, and two *precessions*. Those three are the most noticeable such phenomena. Other planets like Jupiter, Mars, and Venus play minor but noticeable roles still. The said celestial phenomena, and some others, cause periodic (therefore constant) changes on Earth. That makes them

convenient as natural clocks, meaning they provide us with **unity motions**. A unity motion is a fundamental measure of dynamical change, and it means that the actors that carry a change always go back to where they started. This repeatable behavior makes their affairs predictable, so we can measure when a deformation that they caused — therefore itself periodic — completes once.

A **nutation cycle** of 18.6 yr is the time for the actual celestial pole to circumnavigate the mean pole once and is of no concern in this study. The primary or **axial precession cycle**, of $p \approx 26$ ky, is the time for the quasi-conical motion of the mean celestial pole about the ecliptic pole to complete once. The secondary or **apsidal precession cycle** of $p_1 \approx 29$ ky has no dynamical implications in natural spectra other than accompanying the primary-precession's periodicity. An **obliquity cycle** of $p' \approx 41$ ky is the time needed for the varying Earth axial tilt (angle between rotational and orbital axes) to change once. An **eccentricity cycle** of $p'' \approx 100$ ky is the time for deformation in Earth orbit about the Sun (due to divergence of orbital trajectory from a perfect circle) to vary once. **Planetary precession cycles** arise due to the effects of planetary perturbations, primarily by Jupiter and Mars and to a lesser degree Venus and Mercury, on the motions of Earth and Moon. Milankovitch (1941) posited that the above phenomena, over the course of their unity motion, affect Earth's climate.

All of the above-stated periods vary and oscillate in time due to traction by generally unpredictable geophysical and astrophysical forces. Therefore, measuring the actual periodicity of the above astronomical cycles accurately and precisely at any given instant — past, present, or future — requires timing systems of the highest precision. For that purpose, astronomers and geodesists have developed various reference systems, frames, and means. The time systems are **solar time**, based on the Earth revolution about the Sun, and **sidereal time**, based on Earth rotation about its axis. Astrophysical forces affect the former time system mostly and geophysical the latter. While solar time helps us with the calendar and seasons, sidereal time helps us measure the real diurnal (over the course of one day) rotation of the Earth. Therefore, given that the Earth rotation is affected by the above-mentioned astronomical phenomena while the Sun itself is not, sidereal time is more relevant in Earth sciences than solar time is. Specifically, due to precession and nutation, Earth rotation is subject to the motion of the **equinox** — the instant at which the Earth equatorial plane passes through the center of the Sun plane. Thus sidereal time reflects the actual rotation of the Earth, and we can determine it from observations to stars, artificial satellites, and extragalactic radio sources. Then, there is the **apparent sidereal time** that measures Earth rotation with respect to true equinox. Of relevance then is the **apparent diurnal motion** of the Sun — an effect due to both Earth's non-uniform diurnal rotation and its orbital motion about the Sun. For each local meridian, there is always a corresponding local sidereal time. Then, the **local mean time** is a true time at a given location, while the (always local-only) **apparent solar time** is the apparent motion of the actual Sun based on the apparent solar day as a measure of time between two successive returns of the Sun to the local meridian. Likewise, one **solar year** (also called tropical year) measures the time between two successive returns of the Sun to the same position in the sky. While defining our calendars and seasons, it differs by 20 min 24 s from one **sidereal year** that measures the time for the Earth to orbit the Sun once relative to fixed stars.

Of all the above-mentioned astronomical periods, apparent times are virtually (but never absolutely) independent only of precessions. (Seidelmann, 1992) This last point is the motivation behind the minimalistic approach of tying the geological timescales primarily to the precessional cycles. This study addresses the apparent times problem — their previously neglected imperfections in particular and the effects those imperfections have on paleodata analyses. In what follows, *precession resonance* marks orbital resonance, and *precessional resonance* includes energy transfer from an orbital forcing (or disturbances from it) as impressed into solid or gaseous (solidified) matter that had recorded it or otherwise given in to it. The energy transfer also causes classical *mechanical resonance* — the phenomenon of resonating vibration of matter, notably solids, occurring when the natural

period of oscillation of a body of mass coincides with a period of oscillation (or its fractional multiple) of another body of mass. A *subharmonic mechanical resonance* occurs when the matched period represents a subharmonic nonlinear vibration $n/(mT)$; $n \in \mathbb{N}$, $n/m \in (0, 1)$; $n > 1 \wedge n \in \mathbb{N}$. In macroscopic physical systems, such as the Solar system and its objects individually, orbitally forced mechanical resonances can give rise to the *Faraday instability* — a phenomenon characterized by polygonal morphology and patterned topographies. See Omerbashich (2020a) for details on mechanical resonances throughout the Solar system.

I term astronomical cycles and respective periods of duration interchangeably throughout.

3. Methodology

To examine the effects of astronomical forcing on paleodata, I spectrally analyze age calibration of the currently accepted timescale of geomagnetic polarity reversals, spanning the Cenozoic (0–84 My ago) — the revised Geomagnetic Polarity Time Scale 1995 (CKGPTS95; also cited in the literature as GPTS-95) by Cande and Kent (1995), Table 1 and their Table 1. The CKGPTS95 calibration leans on the South Atlantic Anomaly (where the strength of the geomagnetic field is decreasing most rapidly) sequence and consists of nine control points adjusted astrochronologically. At the control points, the sedimentary record is tied to the astronomical record (Hilgen, 1991) so that the CKGPTS95 has excellent sensitivity primarily to the Earth's (theoretical) 25.7-ky axial precession (Shackleton et al., 1990) and possibly to the ~28-ky (apsidal) precession as well (Hilgen, 1991), while tuning to an eccentricity cycle of 412.9-ky was also performed, which was unlike values other workers used (Puetz et al., 2016). As embedded in the timescale itself, the so boosted (systematic) signal becomes an integral part of the overall spectral information, thus easing energy-band (variance-) stratification and enabling separation of actual astronomical periods from any (individually relatively weak) harmonics. Besides, the CKGPTS95 has stood the test of time with its peers, unlike any timescale.

Table 1. Age calibration points for two related geomagnetic polarity timescales extending to end-Campanian. Left panel: for the currently accepted timescale CKGPTS95 (Cande and Kent, 1995). Right panel: for the superseded timescale CKGPTS92 (Cande and Kent, 1992). The facts that calibration points are the most accurate representation of a geological timescale, that CKGPTS95 has stood the test of time like no other timescale, and that the Gauss–Vaníček Spectral Analysis (GVSA) can draw the most accurate spectra from only three values — are used in this study to investigate relations among astronomical forcing and reflections or harmonics recorded in paleodata.

| CKGPTS95 | | | CKGPTS92 | | |
|----------------|----------|------------------------|----------------|----------|------------------------|
| Polarity Chron | Age [My] | S. Atlantic dist. [km] | Polarity Chron | Age [My] | S. Atlantic dist. [km] |
| C3n.4n(o) | 5.23 | 84.68 | C2An(0.0) | 2.60 | 41.75 |
| C5Bn(y) | 14.80 | 290.17 | CSBn(0.0) | 14.80 | 290.17 |
| C6Cn.2r(y) | 23.80 | 501.55 | C6Cn,2r(0.0) | 23.80 | 501.55 |
| C13r(.14) | 33.70 | 759.49 | C13r(.14) | 33.70 | 759.49 |
| C21n(.33) | 46.80 | 1071.62 | C21n(.33) | 46.80 | 1071.62 |
| C24r(.66) | 55.00 | 1221.20 | C24r(.66) | 55.00 | 1221.20 |
| C29r(.3) | 65.00 | 1364.37 | C29r(.3) | 66.00 | 1364.37 |
| C33n(.15) | 74.50 | 1575.56 | C33n(.15) | 74.50 | 1575.56 |
| C34n(y) | 83.00 | 1862.32 | C34n(0.0) | 83.00 | 1862.32 |

I deal with bands from just above the Earth's ~26 ky precessions down to 40 My since astronomical timescales (cyclostratigraphy-based numerical timescales) are reasonably well established for much of Cenozoic time — from the beginning of the Oligocene (~34 My) to the present — while older parts of the timescale have less-complete disconnected cyclostratigraphies that have been referred to as "floating astrochronologies" (Tanner and Lucas, 2014). Besides, beyond 40 My, the accuracy of astrochronological timescales critically depends on the correctness of orbital models and radio-isotopic dating techniques; see, e.g., Westerhold et al. (2012; 2015).

To obtain the periodic signal, I use the Gauss–Vaníček rigorous method of spectral analysis (GVSA) by Vaníček (1969, 1971). The GVSA belongs to the least-squares class of spectral analysis techniques, has many advantages over the Fourier class of spectral analysis techniques in analysing sparse natural data of long spans (Press et al., 2007), and has proven itself by providing absolute extraction accuracy in analysing even extremely gapped paleodata (extinction) records (Omerbashich, 2021, 2006, 2007b). A GV (Gauss–Vaníček) spectrum, s_j , is obtained at a spectral resolution k (here 1000 spectral values throughout), for k corresponding periods T_j or frequencies ω_j and output with spectral magnitudes M_j , as:

$$s_j(T_j, M_j); \quad j \in \mathbb{Z}, \quad j = 1 \dots k \quad \wedge \quad k \in \aleph. \quad (1)$$

In its simplest form, i.e., when there is no *a priori* knowledge on data constituents such as datum offsets, linear trends, and instrumental drifts, a GVSA spectrum s is computed as (Omerbashich, 2004):

$$s(\omega_j, M_j) = \frac{\mathbf{l}^T \cdot \mathbf{p}(\omega_j)}{\mathbf{l}^T \cdot \mathbf{l}}, \quad (2)$$

obtained after two orthogonal projections. First, of the vector of m observations, \mathbf{l} , onto the manifold $Z(\Psi)$ spanned by different base functions (columns of \mathbf{A} matrix) at a time instant t , $\Psi = [\cos \omega t, \sin \omega t]$, to obtain the best fitting approximant $\mathbf{p} = \sum_{i=1}^m \hat{c}_i \Psi_i$ to \mathbf{l} such that the residuals $\hat{\mathbf{v}} = \mathbf{l} - \mathbf{p}$ are minimized in the least-squares sense for $\hat{\mathbf{c}} = (\Psi^T \mathbf{C}_l^{-1} \Psi)^{-1} \cdot \Psi^T \mathbf{C}_l^{-1} \mathbf{l}$. The second projection, of \mathbf{p} onto \mathbf{l} , enables us to obtain the spectral value, Eq. (2). Vectors $\mathbf{u}_j = \Psi^T \Psi_{NK+1}$ and $\mathbf{v}_j = \Psi^T \Psi_{NK+2}$, $j = 1, 2, \dots, NK \in \aleph$, compose columns of the matrix $\mathbf{A}_{NK, NK} = \Psi^T \Psi$. Note here that the vectors of known constituents compose matrix $\widehat{\mathbf{A}}_{m, m} = \widehat{\Psi}^T \widehat{\Psi}$, in which case the base functions that span the manifold $Z(\Psi)$ get expanded by known-constituent base functions, $\widehat{\Psi}$, to $\Psi = [\widehat{\Psi}, \cos \omega t, \sin \omega t]$. For a detailed treatment of GVSA with known data constituents, see Wells et al. (1985). Subsequently, the method got simplified into non-rigorous (strictly non-least-squares) formats like the Lomb-Scargle technique created to lower computational burden of the Vaníček's pioneering development, but which no longer is an issue. At the same time, the conventional Fourier transform and spectrum are just special cases of a more general least-squares formulation (Craymer, 1998).

As mentioned, the GVSA provides total (absolute) accuracy in extracting periods from natural data sets — meaning to the prescribed accuracy of analyzed data themselves — of twice the sampling step or data accuracy (Omerbashich, 2007a; 2020a; 2020b). Fed raw data, the GVSA outputs spectral peaks with magnitudes in variance percentages (var%) against linear background noise levels, or in dB (Pagiatakis, 1999). This type of processing enables relative spectral computations, whose results for physical systems are then variance- (directly energy-) stratified. This procedure is unlike that of any other spectral analysis method. Examples of relative types of analyses that the GVSA thus enables include: detecting field dynamics (Omerbashich, 2006; 2003), separation of forcers from

their harmonics, suppressing select periods to reveal underlying dynamics, and computing spectra of spectra to separate overlying dynamics from the respective system that is already dynamical. I use this multifaceted ability of the GVSA to separate harmonics from their drivers and identify oscillation triggers.

GVSA is strict in that, besides estimating a uniform spectrum-wide statistical significance in $\text{var}\%$ for the desired level, say 95%, in a spectrum from a time series with m data values and q known constituents as $1-0.95^{2/(m-q-2)}$ (Steeves, 1981) (Wells et al., 1985), it also imposes an additional constraint for determining the validity of each significant peak individually — the fidelity or realism, Φ . Fidelity is a general information measure in advanced statistics based on the coordinate-independent cumulative distribution and critical yet previously neglected symmetry considerations (Kinkhabwala, 2013). In communications theory, fidelity measures how undesirable it is (according to some fidelity criterion we devise) to receive one information when another information is transmitted (Shannon, 1948). In GVSA, fidelity thus is defined in terms of the theory of spectral analysis as a measure of how undesirable it is for two frequencies to "coincide" (occupy the same frequency space of a sample). A value of GVSA fidelity then is obtained as that time interval (in units of the timescale of the time series analyzed) by which the period of a significant spectral peak must be elongated or shortened to be π -phase-shiftable within the length of that time series. As such, Φ is a measure of the unresolvedness between two consecutive significant spectral peaks (those that cannot be π -phase-shifted). When periods of such spectral peaks differ by more than the fidelity value of the former, those peaks are resolvable. As the *degree of a spectral peak's dependence or tendency to cluster*, this criterion reveals whether a spectral peak can share a systematic nature with another spectral peak, e.g., be part of a batch or an underlying dynamical process like resonance or reflection. The spectral peaks that meet this criterion are in the LSSA software output listed among insignificant, and the rest among significant (hereafter: *physically-statistically significant peaks* or just (fully) *significant peaks* for short).

In this study, input data are then used in their raw form, i.e., without preprocessing such as dataset padding or any types of filtering (including windowing or tapering). All of those operations historically were designed to overcome drawbacks of classical methods such as Fourier's. Finally, I apply no post-processing, used by some to enhance spectra. The declared precision of the here estimated periodicity is ± 10 years throughout. While the minimum number of values the GVSA can extract a spectrum from is three, Table 1, the method does not depend on the Nyquist frequency (Craymer, 1999).

The above factors, combined with unprecedented abilities of the GVSA, such as handling of extremely ($>99.99\%$) depopulated records in their raw form with ease and extracting both field dynamics and over-dynamics (dynamics of dynamics), made the CKGPTS95 the most suitable gauge for examining effects that astronomical cycles and their modulations have on paleodata timing methods and consequently on any other natural periodicity in those data as well. Thus, separating those two types of periodicity (in timescale; in paleodata) should be possible using the GVSA.

4. Probing CKGPTS95 timescale of geomagnetic polarity

The GVSA of the CKGPTS95 nine calibration values, Table 1, has revealed two 99%-significant periods in the 0.02–40.00-My full band: the Earth's axial precession, $p = 25.00$ ky (theoretical median 25.77 ky), and the Earth's apsidal precession, $p_1 = 29.81$ ky (theoretical maximum 29.00 ky), Fig. 1. The $p = 25.00$ ky is the strongest and statistically most significant period found in this study; Olsen (1986) reported the same axial-precessional value in the large-lakes sedimentary record, and it often is used to tune geological timescales astronomically, thereby methodologically (artificially) boosting its power but not overwhelmingly, i.e., not absorbing the power of other periodicities to suppression below significance. Thus, and as desired of a conventional quality timescale, there were no other

99%-significant periods in the 1–40-My narrowed band, which, however, did contain 10 peaks significant at 95%, Fig. 2. The longest was $P = 9.34737$ My, while the remaining 9 are its reflections ordered in a series $P_i = P/i$, $i = 1, \dots, n$; $n \in \mathbb{Z}^+$.

The $P = P_1$ itself is the same peak detected recently by Omerbashich (2021) from the non-marine tetrapods extinctions record, here particularly suitable due to its insensitivity to the ocean-tidal component as the most persistent systematic noise constituent. Thus, P turned out to be just a circular (2π -) modulation of the axial-precessional period, p . Namely, from the vector representation of harmonic oscillation (Den Hartog, 1985), for the 1-yr base oscillation in case of the Earth, one obtains theoretically: $P_{\text{theor}} = 360^\circ \cdot p_{\text{theor}} = 9.27792$ My; $p_{\text{theor}} = 25.772$ ky, which is matched by the here measured P , to within 7% or 69.45 ky or $\sim 2.7 \times$ precession (or approximately twice the CKGPTS95 tuning accuracy, of one precession cycle).

This highly precise computation of a resonant response and its driver (both the enhanced p and naturally arising 2π -phase-shifted p) is yet another demonstration of the ability of the GVSA to extract spectra with the absolute facility (of twice the data accuracy), even from very long-spanning and heavily gapped records of data. Note that the commonly understood statistical fidelity threshold indicating a physical process is $\phi = 12$ (Omerbashich, 2006). If most of the system periods obtained from sparse data were previously reported or are otherwise known as natural periods (astronomical or physical) or their phase-shifted or time-symmetrical modulations (multiples or fractions), then of interest is relative ϕ primarily.

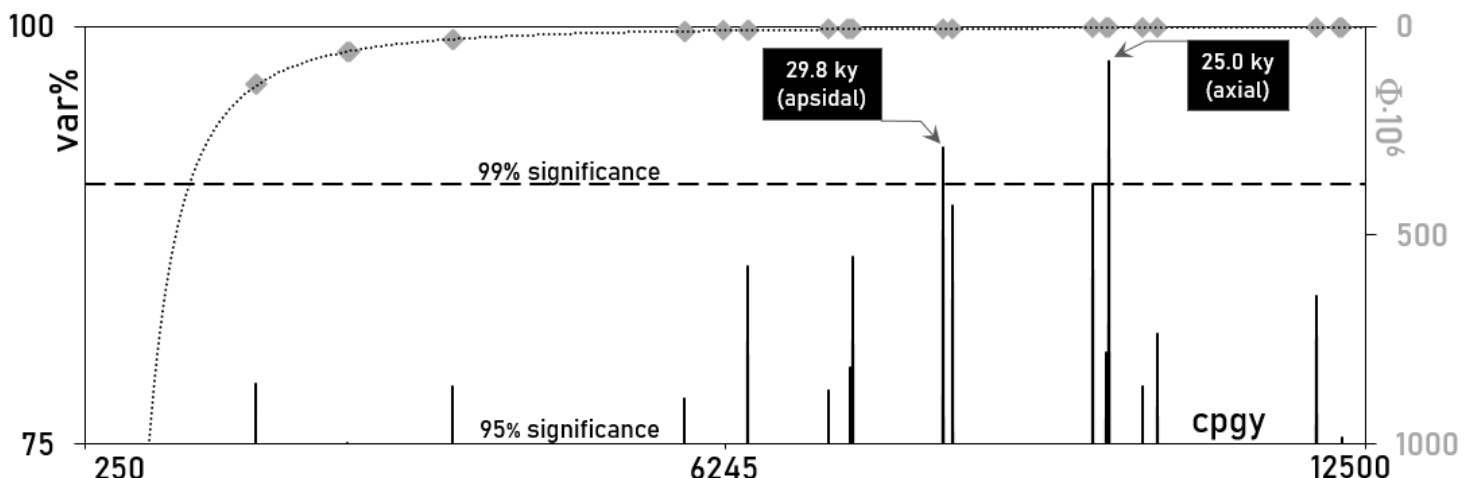


Figure 1. Gauss–Vaníček (GV) spectrum of the currently accepted geomagnetic polarity timescale CKGPTS95 (calibration), Table 1, in the 20 ky–40-My full band. The only 99%-significant periods are the apsidal-precessional, $p_1 = 29.81$ ky (theoretical maximum 29.00 ky), and the axial-precessional, $p = 25.00$ ky (theoretical median: 25.77 ky). Spectral peaks' respective statistical fidelity values are shown overlaid with power trend. Frequencies as depicted here and throughout given in cycles per galactic year, c.p.g.y. (here 250 My).

Mathematically suppressing, see, e.g., Taylor and Hamilton (1972) and Wells et al. (1985), i.e., ignoring (thereinafter enforcing) the axial-precessional period as realized by CKGPTS95, of 0.02500 My, and apsidal-precessional period, of 0.02981 My, made them both disappear below the 99%-significance level, enabling a separation of the two respective groups of reflections as well, Fig. 2 (shows 1–40 My narrow band, no enforcing). The G-V spectra of the now superseded timescale CKGPTS92, previously created by Cande and Kent (1992), contained in the 0.02–40-My full band the 0.025-My axial-precession pe-

riod, its 0.02401-My reflection, and the overestimated 0.03863-My apsidal precession period — all three at the 99%-significance level and with negligible fidelities $\phi < 10^{-5}$. At the 95%-significance level, the superseded GPTS92 timescale was also found periodic in the 1–40 My long band, again with the $P = 9.34737$ -My circular precessional modulation, whose fidelity was a still low $\phi = 0.5$. However, there detected were five reflections, all disordered: 4.31208 My with $\phi = 0.1$, then 4.13793 My with $\phi = 0.1$, 1.72606 My with $\phi = 0.02$, 1.64831 My with $\phi = 0.02$, and 1.40048 My with $\phi = 0.01$.

Finally, the GV spectrum of the current timescale CKGPTS95 in the 40–80-My extended band contained no peaks at any level of significance. Note here that enforcing does not mean a literal data intervention, as no data get removed. Rather systematic contributions (influences) of select periods are suppressed (Wells et al., 1985) via the process of enforcing selected periods. When additional systematic information is sought, which is presumed to underlie an already systematically dominated record of interest, then the residual time-series (enforcing leftover) too can be spectrally analyzed. This procedure can expose secondary dynamics hidden due to the record’s dominant periodicity, like resonance.

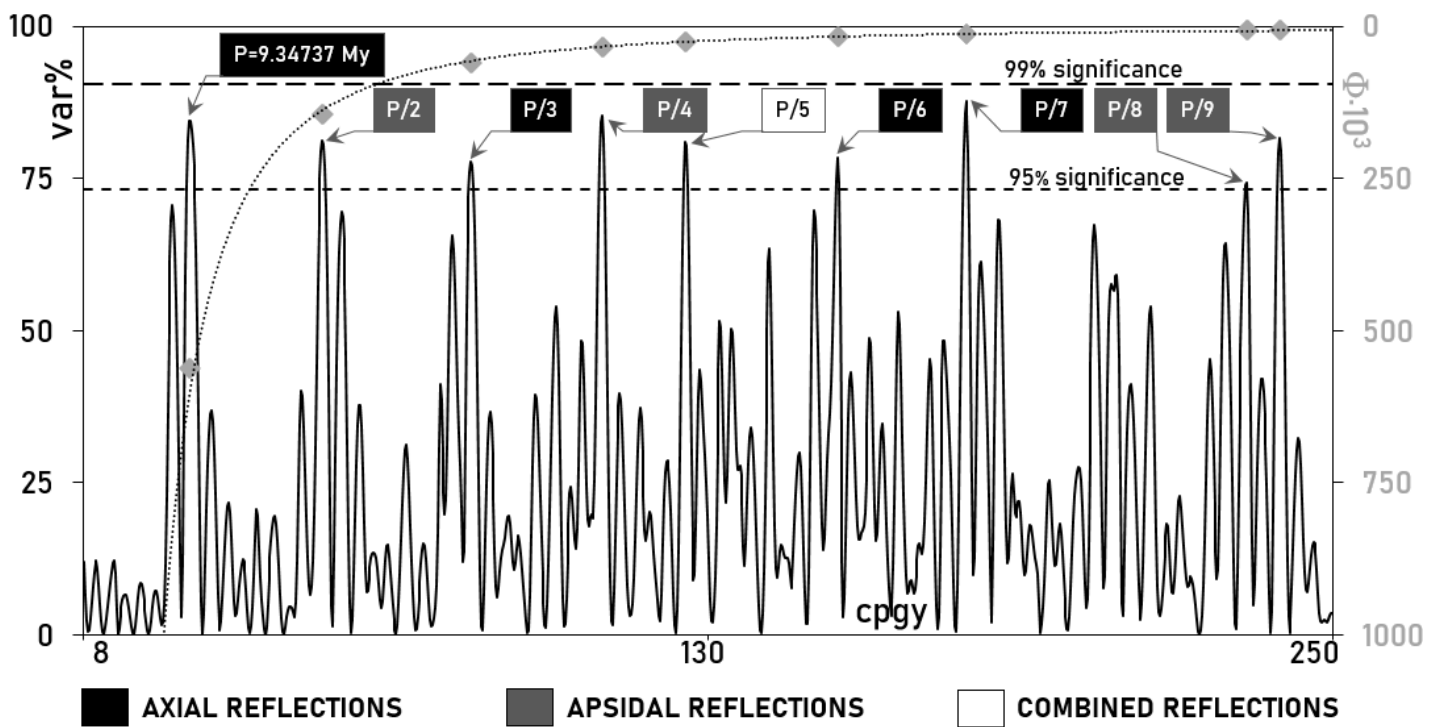


Figure 2. GV spectrum of the currently accepted geomagnetic timescale CKGPTS95 (calibration), Table 1, in the 1–40-My long band, from raw data (no preprocessing including any padding, filtering, or tapering). There are no 99%-significant spectral peaks, as expected after narrowing the band, which has left out the only two 99%-significant periods from the spectral band of interest, Figure 1, as they both are < 1 My. At the 95%-significance level are the lead (main) modulation $P = 9.34737$ My, and its all eight fractional harmonics ($2\pi/n$ modulations of the axial precession), ordered in a series $P_i = P/i$, $i = 1, \dots, n$, Table 2. Further analysis, in which axial- and apsidal-precessional periods get mathematically suppressed, e.g., Taylor and Hamilton (1972), i.e., ignored (thereinafter: enforced), has enabled the separation of the reflections, revealing four of nine periods as predominantly axial precession’s reflections and four apsidal precession’s reflections, respectively. One of the reflections turned out to be due to a combined effect of the two precessions. As in Figure 1, the respective statistical fidelity values for spectral peaks are shown with the power trend overlaid.

Table 2. 95%-significant periods, Figure 2, detected in the 1–40-My-band GV spectrum of the CKGPTS95 geological timescale calibration, Table 1. All turned out to be harmonics of the lead period, $P = 9.34737$ My, itself a 2π (circular) modulation of the precession cycle, $p = 25.772$ ky to within 7‰. The precession's circular (annual-secular) modulation is reported often in the literature, from paleodata of seemingly unrelated types. The statistical tests show that practically there are no outliers (at 1σ) and that all of the series constituents as extracted belong to the same population, i.e., an underlying physical process. Note that, while the here detected ensemble (train) of periods represent harmonics of P , at the same time, they represent reflections of p , so that the two labels are used interchangeably in this study, depending on which of the two lead periods' role needs emphasis.

GVSA of geological timescale CKGPTS95 calibration, 95%-significant periods (1–40-My band)

| i | GVSA period P_i [My] | Φ_{period} | mag [var‰] | harmonic | $\text{theor}P_i = P / (i+2)$ [My] | $\Delta_i = P_i - \text{theor}P_i$ [My] | Δ_i [%] | mean $P - P_i$ [My] |
|---|---------------------------|------------------------|---------------|----------|---------------------------------------|--|-------------------|------------------------|
| | 9.34737 | 0.56000 | 84.52 | P | theoretical: | | difference: | |
| 0 | 4.73011 | 0.14000 | 81.18 | P/2 | 4.67368 | -0.05643 | -1.21 | -2.57071 |
| 1 | 3.05295 | 0.06000 | 77.71 | P/3 | 3.11579 | 0.06284 | 2.00 | -0.89355 |
| 2 | 2.32542 | 0.03500 | 85.36 | P/4 | 2.33684 | 0.01142 | 0.49 | -0.16602 |
| 3 | 2.02247 | 0.02600 | 80.97 | P/5 | 1.86947 | -0.15300 | -8.19 | 0.13693 |
| 4 | 1.62996 | 0.01700 | 78.41 | P/6 | 1.55789 | -0.07207 | -4.63 | 0.52944 |
| 5 | 1.40048 | 0.01300 | 87.72 | P/7 | 1.33534 | -0.06514 | -4.88 | 0.75892 |
| 6 | 1.07108 | 0.00740 | 74.19 | P/8 | 1.16842 | 0.09734 | 8.33 | 1.08832 |
| 7 | 1.04274 | 0.00700 | 81.58 | P/9 | 1.03860 | -0.00414 | -0.40 | 1.11666 |
| mean $P = 2.15940$, $\sigma_P = 1.23872$, 2t-test P_i to $\text{theor}P_i$: 0.9716, F-test P_i to $\text{theor}P_i$: 0.9891. Practically same population. No outliers (1σ) | | | | | | | | |

The above probe greatly justifies the superseding of the GPTS92, as subsequently done with the CKGPTS95 by Cande and Kent (1995). While the current timescale, as tuned so well to Earth precession cycles, has led many also to confuse astronomical periods' adynamical (relatively low-energy) reflections for dynamical (relatively high-energy) periodicity, it nevertheless enables pinpointing the culprit, Fig. 2 and Table 2. Note here that, in addition to neglecting to account for reflections as such, one of the main reasons for reflection periods passing for physical cycles lies in an inherent inability of the Fourier and many other methods of spectral analysis to correctly estimate the statistical significance of spectral peaks (Erlykin et al., 2017, 2018). Modern geological timescales that are tuned astronomically — to orbital frequencies primarily — have, with their systematically erroneous nature, hindered paleodata-based quantitative studies of the already obscured role of those same phenomena (precessions primarily) in the origination of global geo-physical phenomena like the geomagnetic reversals and Milankovitch theory of astronomical forcing of Earth climate. So for example, many who suppress (in the above-described or some other way) the known systematic constituents in the signal, such as the precession, p , do so thinking it would be beneficial in absolute terms. They forget that by doing so, they also destroy or damage any harmonic signal associated with the suppressed constituent. However, such associated co-signals are far from being useless, say when we are looking for the harmonic response of a system to external periodic forcing.

5. Origin of 2π phase-shift

As shown in the above, the P-modulation of p is a phase-shift by the annual base or full circle, 2π . This unity-timer phasing tuned to annual repetitions of some parameter of the Earth-Moon-Sun orbital system indicates that the origin of the shift as recorded by paleodata is in annual variations of some of the time systems that are already inherently inconsistent due to differences from interactions between Earth rotation and revolution.

Orbitally forced climate oscillations are recorded in sedimentary archives through changes in sediment properties, fossil communities, chemical, and isotopic characteristics. (Gradstein et al., 2004) Therefore, the impressing mechanism here is simple: the imprinting itself is always and only done by way of annual cycles and, as such, is subject to any annually injected variations in time systems. Specifically, the time system variation reflective of such variations is the equation of time — itself the annually varying difference between local mean time and apparent solar time (Seidelmann, 1992). The equation of time depicts an effect that arises due to the inclination between the planes of the ecliptic and equator (i.e., the obliquity cycle) and the eccentricity of Earth orbit, i.e., non-uniformity in the apparent motion of the Sun around the ecliptic (i.e., the eccentricity cycle).

The equation of time varies through the year in a smoothly periodic manner by up to 16 minutes, Fig. 3, cumulatively introducing secular variations of the equation of time into the celestial clockwork. Modern geological timescales are tuned to precessions primarily, and obliquity and planetary precessions as secondary gauges. However, the equation of time is virtually independent of precessions, and therefore mainly unaccounted for by timescales. The minimal discrepancies in timing project annually-secularly in a smoothly changing fashion onto incompatible timescales, year after year, century to century, and ad infinitum. When observed as an annual-only phenomenon, i.e., without duration extending to infinity, those changes appear as earthbound (seasonal). However, observed over geological time scales, their true nature as the desynchronization origin becomes clear from Fig. 3. This poorly understood phenomenon is in various versions described in the literature under many names (as an indication of confusion it created), such as precession index, precession-eccentricity syndrome, and many others; see, e.g., Hinnov (2013) for a long list. However, as shown here, the issue is due to the annual variation in the equation in time, Fig. 3, affecting the paleodata sampling process, rather than being due to seasons which is an oversimplification.

That the reflections of the resulting resonant response of the Earth to astronomical forcing indeed tend freely to infinity as expected in an unfixed oscillating system like the Earth-Moon-Sun, can be seen from the above observation of translation symmetry in paleodata in the ~ 30 – ~ 1600 My band (Prokoph and Puetz, 2015). Observed were (Faraday instability ripples in the form of) tripling, doubling, and halving of reflections, their reflections, and reflections of the period reflections. Further rippling likely is undetectable since buried in long-periodic geophysical background noise. As expected again for the above-stated reason, this echo practically extends over the entire geological record, i.e., since the Earth acquired the Moon, ~ 4450 My ago. Thus, what I found above in the 1–40 My band (from arguably the best available data reaching ~ 80 My in the past) should be observable in other 40-My-wide bands, pending quality data from earlier epochs. While Puetz et al. (2014) gave examples of period modulations in paleodata across a variety of scales, including ky small scales, Omerbashich (2022; 2020b) reported a Moon-driven, $>\text{M6.3}$ -seismogenic resonance on the hr-day scales as well and showed that a resonance response of Earth to external periodic forcing is detectable and mappable as actual waves in solid matter passing through continuous-GPS (cGPS) stations.

As a paleosample returns along with the Earth once a year to its original position as when created, its physical state (more precisely: its relation to physical parameters in the local environment as traced by sidereal time) does not. Instead, the sample's physical state changes each year ever so slightly due to astronomical cycles other than precession, only to return to the original state (from the epoch when first created) after a full precessional cycle of 26 ky. By that time, however, this variation had impressed a cyclicity in the samples, along with the phasing appearance of its accompanying modulations (mathematical repetitions). As a result, data of mutually diverse types (cratering, deep cores, fossils, magnetic field, sediments, etc.) and from all epochs return same astronomical reflections regardless if the data were forced by the same astronomical period themselves. However, those periods largely do not reflect the times of samples creation, but the conditions under which the samples had been relating to their year-to-year successive physical states with respect to original local environments as traced by sidereal and apparent times. The longer the data span, the more enduring the impression, so that in Earth polarity records for example, the P-reflections clusters are seen only in the long band, as they tend towards the lower frequencies, Fig. 4 (bar line).

Unlike with the above-described mechanism for impressing reflections (mainly trailing, i.e., harmonics with higher-order indices), the action by the most energized part of a (by now mechanical) resonance — the driver and its first few harmonics (with lower-order indices) — requires a carrier wave. Carrier waves can deliver cumulative effects of the resonance's destructive angular deflections, crashing into obstacles such as variations in topography and crustal thickness — radially, and along all the propagation paths of the resonance as a whole.

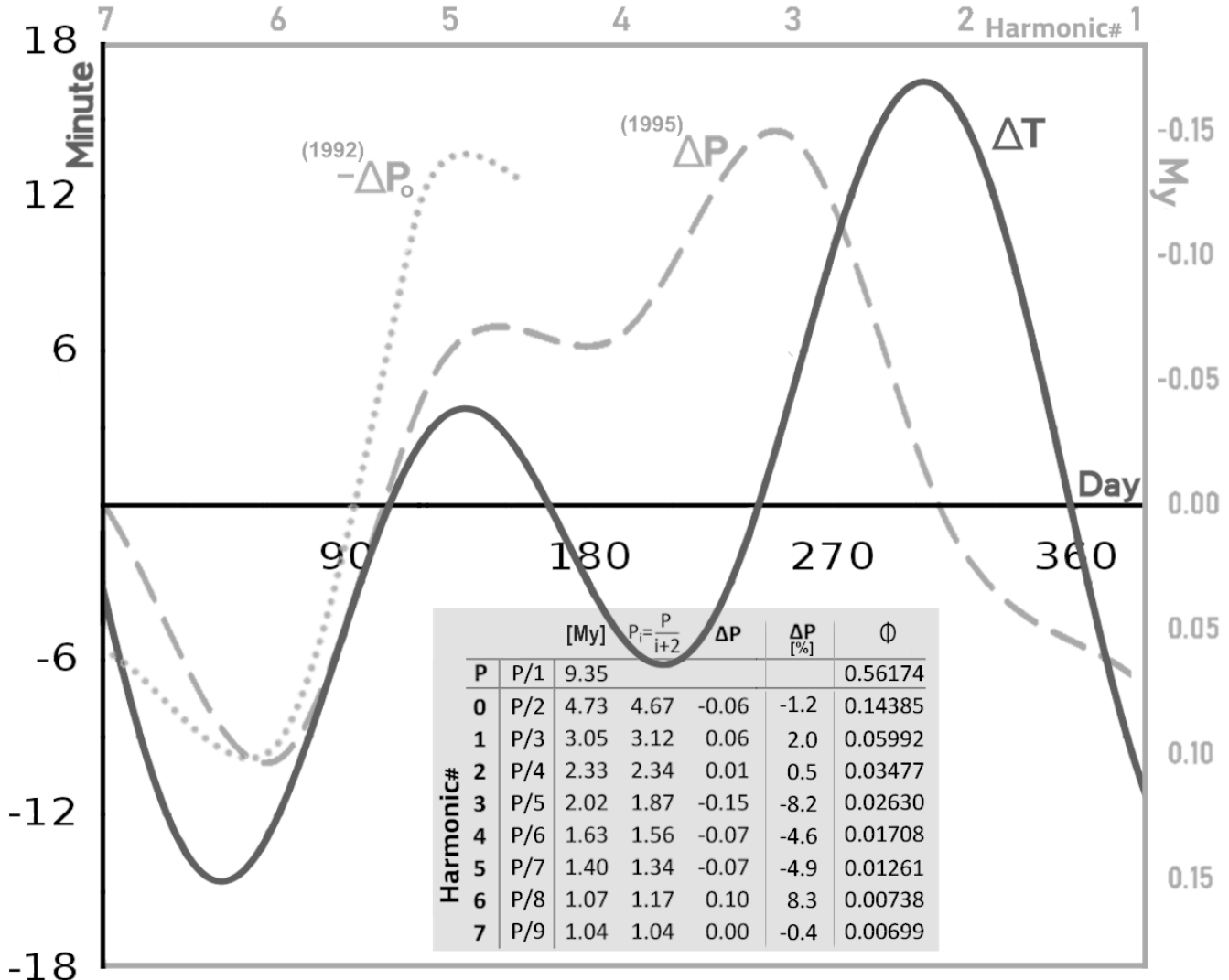


Figure 3. Cumulative projector effect of initial annual timing discrepancies (equation of time variation ΔT , Seidelmann, 1992), solid line, over galactic timescales (long-periodic change ΔP), dashed line. ΔP measures the cumulative change in the ability of paleodata to maintain a theoretical harmonic periodicity with apparent time. The plotted $\Delta T - \Delta P$ consistency (but also the consistency $\Delta T_i / \Delta T_{i+1} - \Delta P_i / \Delta P_{i+1}$, not shown), along with statistics of the matching, Table 2, revealed that the extracted periods belong to a single process, i.e., represent an ensemble of resonance waves. Annual variations in the equation of time are due to imperfections in apparent times and to astronomical phenomena other than precessions, primarily the obliquity (which then is a candidate for resonance trigger). Projector errors largely depend upon the initial conditions under which the entrainment has originated and then locked, so paleodata periods' errors reflect those flaws. Inherent CKGPTS95 errors are also due to phase relations between sedimentary captured and astronomically forced timing always being approximate and known accurately only for the last 5–10 My (Hilgen, 1991). Note accumulation itself occurs alongside neither of the axes, i.e., neither in period nor magnitude. Instead, accumulating occurs across the time domain so that the averaging of the variation as sampled by paleodata for a noticeable spectral change to arise happens already on millennial scales. Therefore, it does not take millions of years for the projector effect to accumulate to a shape resembling that of ΔT , as this occurs already on millennial scales. That is why the higher-order harmonics are approaching ΔT better than lower-order harmonics do. Likewise, the ΔP and ΔT curves eventually coincide for the infinite data span. The superseded CKGPTS92 timescale, ΔP_0 (dotted line), has revealed only the initial ~40% of the projector effect, and therefore performed relatively worse. Besides, enforcing precessional cycles has left no 99%-significant peaks in the GV spectrum of the superseded CKGPTS92.

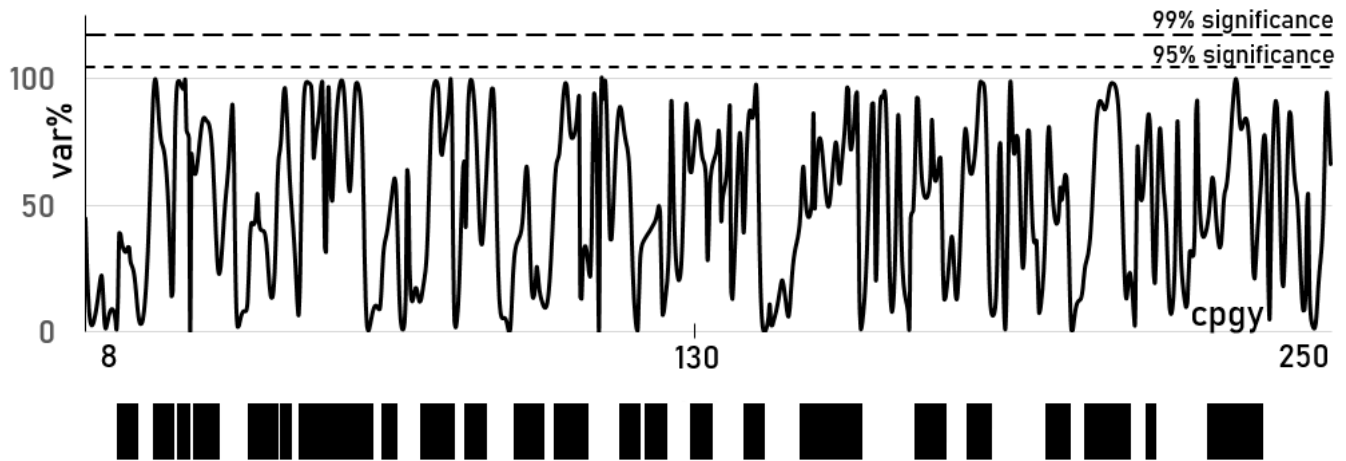


Figure 4. The GV spectrum of CKGPTS95 timescale calibration, Table 1, after enforcing the modulated driver P , Figure 2, and the apsidal-precessional period, 29.81 ky, Figure 1. All 99%- and 95%-significant periods from Figures 1 & 2 vanish below significance. The axial (strongest) precessional period, p , was not enforced, so the spectrum depicts only direct (p -driven) dynamics, as due to precession affecting the reversals, but not due to precessional resonance anymore. As seen from this separation (of a resonance driver from its resonance), since the remaining dynamics is insignificant, the Earth's axial precession alone, with period p , is not responsible for the reversals (sampled by the CKGPTS95 calibration points as the timescale's most reliable portion). However, a uniform background-noise level indicates that another systematic physical process contributes to the dynamics of the reversals. Bar-line: bars width corresponding to local clustering of two or more peaks that did not resolve better than half the spectrum's variance percentage range. The area enveloping white space under a cluster is proportionate to the bar-line blackness and vice-versa. The bar-line depicts the change in clustering with a decrease in period length, indicating that a physical process still underlies geomagnetic reversals, albeit weakly. Systematic noise is seen clustering in the band's low end, dominating the information. Towards the high-end, the systematic noise overpowers all other contents while resolving better (peaks splitting more regularly) due to the absence of other systematic contents.

Any physical system driven by a periodic external field shows a discrete time translation symmetry (Guo et al., 2013). Then rigid subharmonic entrainment can be observed in many-body subharmonic responses (Yao et al., 2020). Such a response is also characteristic of Faraday instabilities (waves or patterns) (*ibid.*), identified by Omerbashich (2020a) as the Solar system's common polygonal (hexagonal mostly) cratering and patterning. Here entrainment means the mode locking between coupled oscillators of different periods, in which they assume a common period (Strogatz, 2000). The Earth's subharmonic response P_i to Earth-Moon-Sun system's orbital dynamics, Figs 1 & 2 and Table 2, is one such entrainment, as seen from the system falling into lockstep with $\frac{1}{4}p'$, or $\frac{1}{4}$ of the obliquity's annually-secularly modulated period rather, P' , Fig. 5. This find confirms the obliquity as (a major) one of the triggers of Earth's resonant response to external (primary tidal) forcing. Other triggers include undulating topography, varying crustal thickness, uneven distribution of inner masses, and mantle flows. Previously, it was believed that such a subharmonic response — with the fundamental frequency's $\frac{1}{4}$ -lockstep to the driver frequency — was characteristic of a discrete (quantum-scale) time crystal only (Yao and Nayak, 2018). However, as shown in this study, (macroscopic) Faraday-instable rigid multi-body systems such as our Solar system exhibit this lockstep too, and its extracted value turned out to be $\frac{1}{4}$ the driver. Puetz et al. (2014) found statistically that the astronomical and geological cycles could be phase-locked synchronously and biological cyclicities lagging, but offered no terrestrial cause.

Additionally, discrete time translation symmetry has been experimentally observed in a resonator forced externally by another quarter-wavelength resonator — both as period multiplication, but mainly as doubling, halving, and tripling (all in parametrically driven tunable superconducting resonators) and as 2π phase shifts accompanied by intensely magnified radiation (in resonators with frequencies $n\cdot\omega$ close to multiples $n = 2, 3, 4$, and 5 , of the resonator's fundamental mode) (Svensson et al., 2018). Besides, a global resonance on Earth occurs when the phase delay owed to propagation is proportional to 2π (Nickolaenko and Hayakawa, 2002). Here, the period multiplication (including doubling, halving, and tripling), the 2π phase shifts (of both p and p'), and the $\frac{1}{4}$ lockstep (to p'), all characterize this study's find from the GVSA of CKGPTS95 calibration, as well. The detection of all three fundamental properties of a discrete time crystal in macroscopic Faraday instability such as the Earth-Moon-Sun system reveals a cross-scale nature of time crystal. The translation symmetry, most often in the form of tripling, doubling, and halving of periods, was previously observed in paleodata in the $\sim 30 \sim 1600$ My band; see, e.g., Prokoph and Puetz (2015), while $\sim 3P$ is often reported in the geophysical literature for 1–40 My band too, most recently by Rampino et al. (2020) as 27.5 My, i.e., 3P to within 2%. However, like with most such reports, that reported period was extracted using inapt techniques (Omerbashich, 2021) that cannot decouple resonances from drivers, resulting in a claim of a physical significance and causality by way of galactic motions, among other proposed but unsubstantiated explanations.

The computations thus far showed that the CKGPTS95 timescale, constructed based on the nine adjusted calibration values, Table 1, is highly accurate. By inclusion, the GVSA of the CKGPTS95 has shown that most inaccuracies in the fundamental radiometric decay constant can be ruled out (Cande and Kent, 1992), except for a systematic error in the decay constants used in K/Ar dating (Hilgen, 1991).

6. Triggering mechanisms

To identify or rule out triggering mechanisms of the precessional resonance as due to orbital forcing (or more precisely, triggers of the Earth's mechanical resonance due to energy-transfer from orbital periods that include direct and mixed effects of orbital resonances), any individual orbital forcing first must be separated. As mentioned earlier, an inherent feature of variance-spectra, used by the GVSA, is a linear depiction of background noise levels. This depiction streamlines relative spectral computations and analyses. In the following, I first separate the drivers from resonance. Then I compute spectra of spectra to separate any overlying and underlying dynamics from the respective system (the entire information contents) that presumably is already dynamical.

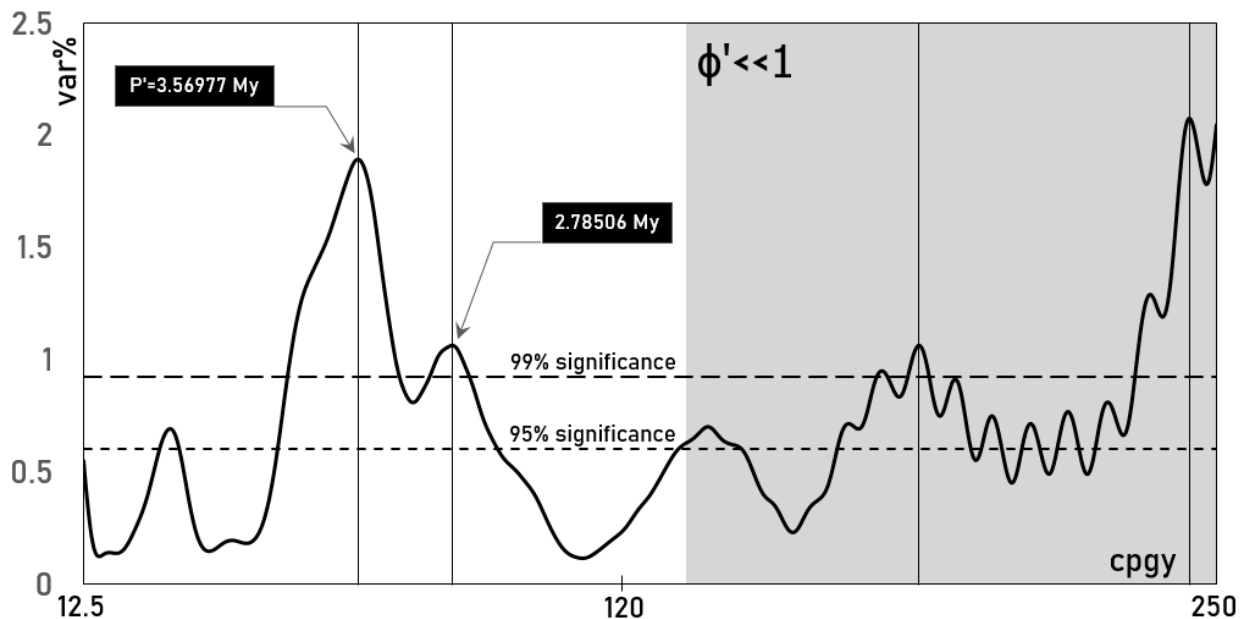


Figure 5. The 1–20-My-band GV spectrum of the CKGPTS95's precession-free spectrum, Figure 4. Only the first two 99%-significant periods are of interest, as indicated by their statistical fidelity. While insufficiently statistically significant to render the two peaks significant physically, the relative variance- (thereinafter: power-) dominance in the $P' = 3.56977$ My period makes it alone the Earth's superperiod (one which controls other periods in a system). Like with the P relative to p , P' also is 2π -phase-shifted, relative to $\frac{1}{4}p'$, which means the Earth-Moon-Sun system fell into the $\frac{1}{4}$ lockstep with the Earth's obliquity that can be viewed then as a co-trigger of the P_i resonance. Unlike a spectrum of a time series, which tells about repetitiveness in data and can thus expose causal physical mechanisms, a spectrum of a spectrum can tell about any repetitiveness of cycles themselves, which can expose overlying dynamics of a system. Such a procedure can have a physical meaning only if dominant dynamics previously are enforced (or ignored, as a more appropriate term given the context). The band was narrowed further, to 1–20-My, as methodologically the strictest approach possible, so to shift the remaining power to the sub-band of interest; this is justified because floating astrochronologies dominate the data beyond the beginning of Oligocene (~34 My) (Tanner and Lucas, 2014).

Enforcing the phase-shifted precessional driver P and the apsidal-precessional cycle p' was sufficient to make all periodicity in the GVSA spectrum of CKGPTS95 vanish below significance, Fig. 4. This vanishing has demonstrated that, according to the CKGPTS95, all dominant (significant) cycles over the past 83 My related to polarity reversals were also related to the precessional resonance but not to the main (axial) precession itself, and there was no secondary field dynamics which precessional resonance dampened. Moreover, the successful separation of the resonance driver from its resonance, Fig. 4, showed that the smallest of disturbances in the precession could also generate the resonance. Finally, the apsidal precession, p_i , could play a role in creating that disturbance and co-triggering the precessional resonance.

This result — that there is no continuous forcing of the reversals, but there are harmonics instead — is supported by Lutz (1985), who found no significant periodicity in geomagnetic reversals and pointed out that long periods in paleodata are either harmonics or not well defined. As astronomical tuning in our case left some room for deciding if the precession causes reversals itself, the uniform (with highest spectral peaks virtually leveled) noise-background level on Fig. 4 reveals the existence of some other systematic modulation that partakes in the dynamics of reversals. An observation of such a modulation mechanism likely would represent the first proof of precessional resonance; see Hin-nov (2013) for a review of (orbital) precession resonance studies. Note here that orbital resonance among heavenly bodies can cross-scale-translate via energy transfer into mass (particle) resonance on the resonantly affected bodies of mass (Omerbashich, 2020a, 2020b).

Carbone et al. (2006) claimed that, based on statistical analyses, a physical process underlies the geomagnetic reversals phenomenon. If indeed real — such a process could also affect measurably the timescale here freed of potentially detrimental effects of astronomical tuning. To test their claim, I use a bar-line descriptor of clustering to plot the change in local clustering with the decrease in period length, Fig. 4. There, as seen from the clustering getting somewhat resolved towards the band's high end, there does appear to be a physical process underlying geomagnetic reversals. Besides, as expected from systematic noise, the spectrum resolves better (with the decrease in period length), i.e., spectral peaks split more regularly towards the high end, to a discernable local declustering that then permeates throughout the highest frequencies as their general tendency towards declustering. Therefore, in addition to the virtual flatness of highest noise peaks, we can see that the systematic noise is not lonely in defining spectral information contents. In short, the clustering does indicate that the noise appears joined by a systematic physical process as well, thus corroborating *ibid.*

To verify this statistical conclusion further, in the physics realm primarily, I compute the spectrum of the spectrum from Fig. 4. Spectra of spectra have been used for a long time (for example, to investigate alternate states of matter, namely in demonstrations of the Bose-Einstein condensate). Computation of the spectrum of a spectrum (rather than comparing individual spectral peaks as done classically) is an inherent ability of the GVSA thanks not only to the method's linear representation of spectral magnitudes but also to straightforward statistical analysis incorporated into the spectral computation itself. In this way, and unlike using statistical approaches alone, such as reanalysing the spectra of post-enforcing residuals, all modulations — including those that arise due to combined effects of two or more periods — can be observed or enforced (ignored) simultaneously. Here the 1–40-My-band spectrum of the same-band spectrum of (now precessions-free) CKGPTS95 can tell us about the dynamics of the process which overlies the geomagnetic reversals, should such a process exist and be systematic (periodic) in its nature. The spectra computed in this study also apply to any future design modifications of the CKGPTS95 and other geological timescales.

The GVSA of the CKGPTS95 (precession-free) spectrum from Fig. 4 has returned in the 1–20-My band spectrum with six peaks significant at the 99% level and eight peaks significant at the 95% level, Fig. 5. The longest 99%-significant peaks were $P' = 3.56977$ My with $\phi = 0.16$, and 2.78506 My with $\phi < 0.1$. Note here a two-magnitudes-of-order overall drop in spectral magnitudes compared to the CKGPTS95 spectrum itself, Fig. 5 v. Figs 1–2 & 4, which makes the $\phi = 0.16$ of P' indicative of a physical process as well, albeit again an adynamical (or relatively low-energy) one. The 3.5-My period was reported first by Olsen and Kent (1999), who also found its $\frac{1}{2}$ harmonic 1.75-My. They identified those cycles in the large-lake sedimentary record and claimed the periods as the first geological evidence of the chaotic behavior of the inner planets. For them, the 1.75-My (3.5-My) does not correspond to anything in the modulation of precession but could be a long-period modulation cycle of obliquity, in which case it must come from indirect forcing (*ibid.*). Indeed, as seen in Fig. 5, the spectrum of the (precessions-free) spectral peaks of CKGPTS95, where timescale periods themselves formed a new time-series largely freed from its conventional astronomical ties, revealed P' as a trigger (indirect forcer) of the geomagnetic reversals record. Note that the obliquity and precession are long considered (semantically) underlying, i.e., controlling variables in the Milankovitch theory as well; see, e.g., Hays et al. (1976).

That P' is another astronomical modulation (now of the obliquity), is seen as before in the case of P (Den Hartog, 1985), so for the 1-yr base oscillation, one obtains theoretically: $\frac{1}{4} \cdot \text{GVSA} P'_{\text{theor}} = 3.56977 \text{ My} / 360^\circ = 9.916 \text{ ky}$, which matches the Earth obliquity's cycle that, as seen here, maintained the lockstep: $\frac{1}{4} P'_{\text{theor}} = 41 \text{ ky} / 4 = 10.250 \text{ ky}$, to within 3.3%. Since P' was obtained indirectly (from spectra of spectra, to free the data trends of the built-in precessions chronology), the normalized achieved accuracy could be up to an order of magnitude better, to around 3%. This possibility also follows from looking at the

period it overpowered, of 2.78506-My, Fig. 5, which itself is 2π -phase-shifted, i.e., a circular modulation of the 3/10 harmonic of theoretical precession $p_{\text{theor}} = 25.772$ ky, i.e., $360^\circ \cdot (3/10)p$, to within just 0.6‰. Excellent matching to the theoretical precession rather than precession realized in the CKGPTS95-adjusted strata is owing to the above-described methodology, namely combined separation of driver from resonance via computation of the spectra of spectra. Additionally, this overpowering of the precession's second-longest and second-strongest phase-shifted modulation by the obliquity's longest and therefore strongest modulation is direct evidence that, in their interplay, it is the obliquity which at least partially controls the precession (and thus indirectly the precessional resonance too), and not the other way around.

Indeed, as seen from Figs 2 & 5, P modulates P_i as a forcer (driver) significantly — so that the P_i are its well-defined harmonics (continuous unity-fractions) rather than reflections (intermittent integer multiples). Then as seen from the spectrum of CKGPTS95 spectrum, Fig. 5, and by sheer existence and placement of the P' , the P' itself is the superperiod (superimposed period) to P and any P -harmonics. This interplay, in turn, means that the obliquity acts on the precession indirectly: due to the projector effect and the resulting phase shift, Fig. 3, P' impresses upon P instead of p' impressing upon either p or p_i (or both). Note here that the detection of a precessional resonance in the 1–40 My band was enabled in part by methodological band-pass filtering of orbital tuning, which modeled noise in the immediate spectral vicinities of p and $\frac{1}{4}p'$ by focusing spectral power from surrounding frequencies to the Milankovitch bands (Hinnov, 2000).

In the same sense, note that the Universal Wave Series (UWS) harmonic periods in the 1 ky–1 My band (Puetz et al., 2016) are a hint at the precessional resonance as demonstrated here to be originating in the 1–40-My band and an independent proof that resonance harmonics generally are recoverable from astronomically tuned timescales. Besides, given the methodology used and the number of calibration points, the P' fidelity normalized to at least an order-of-magnitude-larger value does appear sufficient for P' to be outright called physically significant (dynamical) and for its $\frac{1}{4}p'$ base to be recognized as the cause of the chaotic behavior of the inner planets, as inferred by Olsen and Kent (1999). Also, P' is among the strongest periods found in this study, right after the axial-precessional period, p , and its circular modulation, P . Then after using up all the power in data, P stands out as the lead period to some of the most potent terrestrial cycles. Together with its lower-order resonance harmonics, crosscycles primarily (as due to cross-coupled oscillations; the P -harmonics that at the same time are harmonics of other astronomical cycles and their modulations as well), forcing and transformative potential of the precessional resonance-dynamics on inner planets becomes unquestionable.

7. Milankovitch theory as a special case of Earth-Moon-Sun resonance dynamics

The Milankovitch theory is successful mostly over the Pleistocene, i.e., between 0.01–2.6 My ago (Feng and Bailer-Jones, 2015). From the resonance dynamics perspective, the reason for this is in the Pleistocene fitting the frequencies of tailing long-period P -harmonics, Table 2, causing the most recent precession's 2π (circular) modulation to be confused for the precession's base cycle and the primary (direct) energy-transfer mechanism. In the same sense, however, P and its first few harmonics carry most of the power of Earth-Moon-Sun resonant dynamics, which is why they affect geophysical processes the most. After all, it is P , its first few harmonics, and their various modulations, which get reported from numerous and seemingly unrelated types of paleodata; see, e.g., Rampino and Prokoph (2020) for an overview, and Omerbashich (2021) for a summary of such adynamical periodicity.

As mentioned earlier, besides Carbone et al. (2006) who also saw an underlying process in geomagnetic polarity reversals, Olsen and Kent (1999) previously reported the obliquity periodicity in the geological record. Those two studies then corroborate the here

reported find of a physical process causing the reversals and excursions (incomplete or short-term reversals). Note again that timescales in practice are tied to the precessions primarily (and to a lesser degree eccentricity) because the geological record and other global data do not seem to reflect precession cycles. Similarly, the eccentricity cycle is considered insignificant in comparison to other orbital forcers.

That the results of this study and supporting two studies are correct is seen from certain aspects of the Milankovitch theory, specifically its predictive abilities. For example, the lack of precession in the geological record historically is attributed to the importance of annual insolation (controlled by the obliquity), with more influence on polar temperatures than seasonal insolation (modulated by the precession) (Naish et al., 2009). Therefore, the statistical and physical significances of any obliquity modulations are not immediately discernable either, due to the methodology of designing a timescale, which then has to be undesigned — here by computing spectra of spectra (note that there are numerous other methods too).

Related to that was the above find that the obliquity, non-critically (seen from affecting systematic noise content right below precessional) and indirectly (as overlying other astronomical cycles), partakes in the control of geomagnetic reversals. Then this find also supports the Milankovitch (untestable; see *ibid.*) hypothesis that summer half-year insolation intensity, with its sensitivity to the precession, can control geophysical parameters like the surface temperature and growth and decay of ice sheets. Therefore, the here confirmed 3.5-My cycle is a likely candidate for the Earth's superperiod — a periodicity superimposed on all other periods in a physical system. To show that a superperiod in the latter case has a physical meaning, any adynamical data periodicity and reflections first must be separated from respective drivers. Only after such signal separation, here used to simultaneously remove any effects of the astrochronology from the timescale calibration, can it be expected from the spectrum of a spectrum of that timescale to extract meaningful (dynamics-related) repetitiveness of a data period itself.

Also, the present study supports the Milankovitch theory in that it did not find the 100-ky eccentricity period like that in time-series of ice ages — proclaimed by some as the period Milankovitch theory cannot explain and therefore collapses as a theory; see, e.g., Berger (2012). Moreover, there is no phase-shifted eccentricity either. However, a faint though 99%-significant spectral peak at 100.02-ky with a very high 99.5-var% magnitude but forbiddingly negligible $\Phi = 0.000064$ is seen but only when the upper limit of the spectral band of interest is set very near the precession and obliquity periods, say in-between those at 0.035 My so to cancel out any spectral leakage effects. (For example, setting the band's upper limit just below obliquity as another dominant cycle while leaving the opposite vicinity vacant demonstrates an unmitigated leakage effect: the only 99%-significant peak at 84.02-ky (twice the obliquity to within <2.5%) gets picked up at a very high 93.2-var% magnitude, but again with a forbidding $\Phi = 0.000045$. Thus the obliquity cycle itself leaks beyond detection, and all that is left is its 2T reflection.)

This proven presence of a period only after a deliberate data manipulation identifies the 100.02-ky as an obliquity-precessional resonance period (note its suspiciously round precision too, indicating an artificial, i.e., precession-tuning origin rather than a genuine eccentricity cycle), and shows that its detection by other workers is likely due to data pre-processing including padding, filtering, and tapering. This separation of an astronomical period from a similar but unrelated resonant period was possible thanks to the earlier described and repeatedly demonstrated absolute-extraction abilities of the GVSA from as few as three values.

Insomuch as ice ages and geomagnetism are phenomena not entirely independent, this all-embracing indication at positive verification of the Milankovitch theory is owing to the most profitable use of data by definition of a scientific endeavor: in their raw form. Berger (2012), who used a GVSA variant to compute a short-band periodogram of the geomagnetic record compiled by Bassinot et al. (1994), supports this conclusion. Berger

(2012) thus found no 100-ky period either, while also strongly suggesting significant variation near obliquity and in various lines related to precession (*ibid.*), resembling resonance interplay. This outcome was to be expected if the Milankovitch forcing — and the precession especially — is the Earth's leading dynamical driver, say, of ice mass, see *ibid.*

8. Verification of resonance-moderation of polarity reversals and strata

To verify the above detection of resonance response of the Earth to external forcing due to entrainment and the consequent resonance-moderation of magnetic polarity reversals and strata, I first demonstrate the ability of the GVSA to extract known resonances from paleodata. Subsequently, I show that the Rampino period, P_R , while being the sole and dynamical actor in geomagnetic reversals, belongs to the precessional resonance as well. P_R is a carrier wave of resonance's destructive deflections, indirectly responsible for the polarity reversals by downward penetrating, enveloping the inner core, and eventually flipping the geomagnetic polarity.

8.1. Extraction of previously reported planetary resonances

For that purpose, I compute the 1–40-My-band spectrum of the time series of residuals that have remained after enforcing the precessions in CKGPTS95 calibration. Residual-time-series analysis is another feature inherent to the GVSA, making it a comprehensive numerical-statistical analysis package rather than just a numerical computations algorithm. Here, spectra of a residual time-series can unhide any periods previously suppressed by a systematic signal that is being enforced (Wells et al., 1985). (Note that the entire resonance train gets enforced with enforcing P ; this is another, now methodological, evidence that the ensemble of P_i harmonics as a whole indeed forms the precessional resonance.) Thus the GV spectrum of residuals has revealed 95%-significant known periods of the Earth-Mars planetary resonances recognized earlier in various (mostly older than 83 My) parts of the geological record, now for the first time in the 0–83-My specific part also (see Table 3 of Hinnov, 2013); see Table 3 for complete data.

Table 3. Matching of 95%-significant periods in the 1–40-My-band GV spectrum of CKGPTS95-spectrum's residuals remaining after enforcing P (and thus P_i , too), against the same periods as reported previously; see Table 3 of Hinnov (2013) and Table 1 of Rampino and Prokoph (2020). There were no 99%-significant peaks — as expected after enforcing the dominant precessions and their reflections (precessional-resonance) signals in data naturally dominated by resonances (not just the enforcing-suppressed ones, but also planetary like Earth-Mars). Note a very low statistical fidelity, Φ , on most periods, as indicative of resonant or otherwise mostly powerless spectral periods. Here power is in the sense of relayed energy, not GVSA magnitudes as commonly given in variance percentages (but which can also be expressed in spectral power (spectral density) units of dB, see Pagiatakis, 1999). The CKGPTS95 timescale spans 0–83 My, Table 1.

| Stratigraphic record | Planetary resonance | | GVSA of CKGPTS95-spectrum's residuals (0–83 My), p & P enforced | | |
|---|--|---------------|---|------------------------|---------------------|
| | g4-g3 [My] | s4-s3 [My] | period [My] | Φ_{period} | magnitude [var%] |
| NEOGENE Pleistocene–Miocene (0–9 Ma) $\delta^{18}\text{O}$ sea level Miller et al. (2005); Boulila et al. (2011) | | 1.2 | 1.11905 | 0.00110 | 73.75 |
| MIOCENE-OLIGOCENE (20–34 Ma) Benthic marine $\delta^{18}\text{O}$ Ocean Drilling Program (ODP) Site 1218 Pälike et al. (2006); Boulila et al. (2011) | | 1.2 | 1.11905 | 0.00110 | 73.75 |
| CRETACEOUS Aptian-Albian (100–125 My) Scisti a Fucoidi, Italy Grippo et al. (2004); Huang et al. (2010) | 1.5 | | 1.60695 | 0.00230 | 87.69 |
| TRIASSIC-JURASSIC Norian-Pliensbachian (205–184 My) Inuyama Chert, Japan Ikeda and Tada (2013) | 1.6–1.8 | | 1.60695 1.83749 | 0.00230 0.00300 | 87.69 82.73 |
| TRIASSIC Carnian-Rhaetian (230–200 My) Newark Series, USA Olsen (2010) | 1.7 | | 1.60695 1.83749 | 0.00230 0.00300 | 87.69 82.73 |
| TRIASSIC Anisian-Ladinian (245–237 My) Inuyama Chert, Japan Ikeda et al. (2010) | 1.8 | | 1.83749 | 0.00300 | 82.73 |
| PERMIAN Wuchiapingian-Changhsingian (251–260 My) Wujiaping-Dalong Formations Wu et al. (2013) | | 3.11 | 3.18584 | 0.00910 | 76.29 |
| Compilations | Average lead cycle [My] | | GVSA of CKGPTS95-spectrum's residuals (0–83 My), p & P enforced | | |
| ENDING WITH PALEOPROTEROZOIC Holocene-Orosirian (0–2023 My) Compilation of 58 cratering & 35 mass-extinction reports Rampino and Prokoph (2020) | 26.5 (mass extinctions) ~26 (craters + mass ext.) | | 26.53386 | 0.63000 | 77.02 |
| Various paleodata | period [My] | | GVSA of CKGPTS95-spectrum's residuals (0–83 My), p & P enforced | | |
| PERMIAN/TRIASSIC Holocene-Permian/Triassic (0–253 My) Mass-extinction episodes Raup and Sepkoski (1984) | 26.4 | | 26.53386 | 0.63000 | 77.02 |
| ENDING WITH PALEOPROTEROZOIC Holocene-Orosirian (0–2023 My) Cratering record Chang and Moon (2005) | 26.4 | | 26.53386 | 0.63000 | 77.02 |

8.2. Extraction of periods previously reported from cratering and extinctions

I now extract periods previously reported as dominant in cratering and mass-extinction records. Note that the most significant period revealed from the precession-free geomagnetic reversals CKGPTS95 calibration, of 26.5 My and at a very high magnitude of 77.0 var% with a moderate $\Phi = 0.63$ (nonetheless relatively highest of any period extracted in this study), could not be identified as a resonance reflection or harmonic. This period has been reported previously by Rampino and Prokoph (2020) as the average dominant cycle in a compilation of 58 reports of cratering and 35 reports of mass extinctions and here therefore termed the *Rampino period*, P_R . (Note that Raup and Sepkoski (1984) and Chang and Moon (2005) came significantly close to it from an extinctions record spanning 0–253 My and a cratering record spanning 0–150 My, respectively, Table 3.) Compiled periods were based on many completely different methods and approaches to computing and analysing spectra. This period reveals a powerful wave (the sole and dynamical actor) as it affected solid matter. Besides, it is of the highest fidelity found on any period extracted in this study. Its remarkable power is stressed even further when we know that it took the entire precessional resonance train (ensemble) to hide it.

P_R is so pure and persistent that it even appears as a co-driver of other (the short-period; ky-) harmonics, Table 4. However, it does not emit longer-period harmonics, revealing that the resonance confines it to (many) relatively short intervals of time — disallowing it by the resonant nature of the process itself to be ever encountered by the entire geological record. Since also supported by the combined cratering-extinctions record as well as the extinctions record alone, P_R most likely represents the precessional resonance's crosscyclic (multi-harmonic) carrier of the peak angular deflection. Here cratering is mainly understood as petrified evidence of large-scale polygonal geomorphology seen throughout the Solar system due to the imprinting of actual solid-matter resonance waves via macroscale Faraday latticing into the molten material (melted on impact as well, in a snapshot fashion). In the same sense, originally polygonal crater edges eventually erode into circular (here the most realistic scenario) shapes rather than the other way around, i.e., from circular into polygonal geometries as believed by some (the least realistic scenario); see Omerbashich (2020a).

The decisive role of precessional mechanical resonance for Earth is particularly plausible since found in both the cratering and the calibration as the most accurate portion of the currently accepted (timescale of the) geomagnetic polarity reversals record. These multiple detections from seemingly disparate data mean that the precessional resonance is directly, and the precession and obliquity in tandem indirectly (along with geomorphology varying in crustal thickness in particular, and other causes), responsible for the geomagnetic reversals as well. Finally, Rampino and Prokoph (2020) deduced that records of cratering and mass extinctions are somehow connected. Indeed, their fundamental connection follows from the above result: not only is the precessional resonance long-term destructive (mainly causing geomagnetic excursions — started but never finished reversals — that appear like gradual processes while masking the cataclysmic nature of the reversals) but also strictly terrestrial and incessant. Then the record of mass extinctions is a record of the destruction of evidence of life during Transformative Resonant Events (TRE), instead of periodicity of mass extinctions themselves (note that evidence of only a few remarkable mass-extinction events is beyond doubt). This unavoidable inference questions most if not all past claims of periodic mass extinctions.

The well-established fact that life always appeared to have sprung back incredibly fast following an extinction event (*ibid.*) inevitably reveals the circular logic of the proponents of periodic mass extinctions, making the mass-extinctions records work just the same in the opposite direction too — as evidence of the no-mass-extinction scenario of life on Earth. Besides, the fact that 35 globally random extinction episodes can average to the value of the dominant period of geomagnetic reversals, and a combined record of 35 extinction events and 58 cratering events) within half-order of magnitude so, is remarkable

in itself because it reveals that all three phenomena — polarity reversals, polygonal “cratering”, and “periodic” extinctions are due to a single process. (Here, extinctions are supposed regardless if represented really by the record of extinctions or their sample’s violent decimation such as what large igneous provinces had done to the geological record; see, e.g., Prokoph and Puetz, 2015).

Most importantly, since the average of dominant periods, as returned from globally randomly sampled and diverse data sets, exactly match the dominant periodicity of one of those global phenomena, the underlying physical process then must be ergodic. Thus, there is nothing chaotic about those processes, including the geomagnetic field whose recent ergodicity is established (De Santis et al., 2011). The extraction of the Rampino period then means a data-based confirmation of geomagnetism overall ergodicity.

Table 4. Values of the 95%-significant GV spectral peaks from the 0.02–40-My band of the geomagnetic reversals’ currently accepted timescale, CKGPTS95, Table 1. The 99%-significant periods are plotted in Figure 1. Compared to Table 2, showing the same but in 1–40-My band, the extraction of the above periods was affected by the power of the precession cycle, p , as one of the clearest periods found in this study. The four clusters of split periods are shown as declustered (represented by one period-value per cluster). The above-listed, short (ky-) periods are mostly harmonics of P – circular modulation of precession p ; P' – circular modulation of $\frac{1}{4}p'$ obliquity; and P_R – Rampino period, of 26.5 My (Rampino and Prokoph, 2020). Note that a precessional 20.41-ky period and its 5/2-modulation to within <1%, 50.54-ky, are crosscycles of both Rampino harmonics and precessional circular modulation’s harmonics (indicating that P dominates P_R rather than the other way around). This direct P - P_R connection confirms P_R as most relevant and potent in terms of orbital-mechanical resonance energy transfer. Note that the most efficient feature of mechanical resonance in terms of ability to relay destruction is its magnification effect via frequency demultiplication, which upsurges the energy injected resonantly into a physical system by 100s of times (Den Hartog, 1985).

| GVSA of CKGPTS95-spectrum’s residuals (p and P enforced) | | | harmonic |
|---|------------------------|---------------|-------------------|
| period [My] | Φ_{period} | mag [var%] | |
| 0.14974 | 0.0001400 | 78.61 | |
| 0.09775 | 0.0000610 | 75.07 | |
| 0.06977 | 0.0000310 | 78.46 | $P/134$ |
| 0.06929 | 0.0000310 | 74.59 | $P/135$ |
| 0.06543 | 0.0000280 | 73.49 | |
| 0.05054 | 0.0000160 | 74.34 | $P/185, P_R/525$ |
| 0.04267 | 0.0000120 | 77.72 | $P/219$ |
| 0.04010 | 0.0000100 | 73.32 | |
| 0.03863 | 0.0000096 | 85.65 | $P/242$ |
| 0.03346 | 0.0000072 | 79.57 | $P_R/793$ |
| 0.03334 | 0.0000071 | 86.19 | $P'/107$ |
| 0.02951 | 0.0000056 | 89.23 | $P'/121$ |
| 0.02422 | 0.0000038 | 78.45 | $P/386$ |
| 0.02041 | 0.0000027 | 73.50 | $P/458, P_R/1300$ |
| 0.02037 | 0.0000027 | 75.38 | |

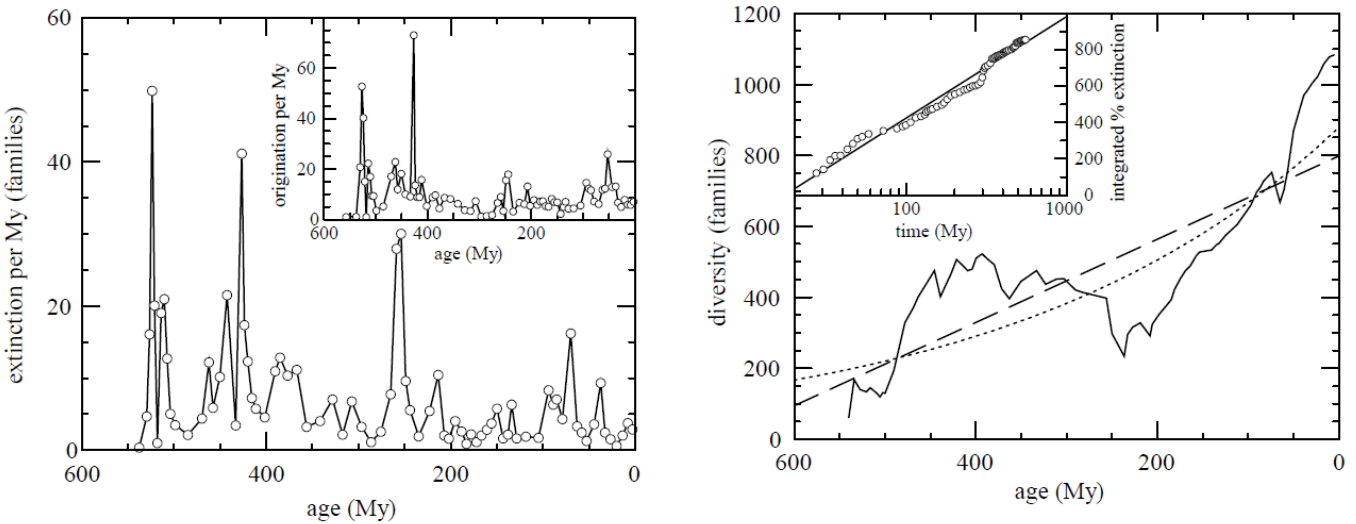


Figure 6. Left panel: Extinction rate in families per My for marine organisms as a function of time; callout: origination rate for the marine organisms. Right panel: the number of known families of Phanerozoic marine organisms, as a function of time (linear trend dashed; exponential trend dashed); callout: the integrated percentage extinction of families. From: Newman and Sibani (1999). Trends are steady but non-monotonic. Note that, due to sensitivity to the ocean tidal component as the most persistent systematic noise constituent, marine genera somewhat exaggerate the trending.

The data of alleged extinctions support this possibility themselves: the average intensity of extinction of marine life during the Phanerozoic has decreased, i.e., changed on a steady downward trend, while the number of families increased unobstructed, Fig. 6 (Newman and Sibani, 1999). It is implausible that most if not all species over time had developed natural resistance of the same kind and at the same level or extent, to the causes of extinction, since that would imply thousands of factors to coincide and remain congruent over half a billion years at least. This steady drop in extinction intensity resembles energy dissipation of an underlying physical process, and the increase in the number of families (and lifespan too, as later studies have shown) correspond to a scenario without any extinctions whatsoever, i.e., as if geophysical upheaval responsible for geomagnetic reversals and cratering has also decimated the record of species but not the species themselves.

The orbital-mechanical resonance due to energy transfer is a process that fits the above description: it naturally dissipates over very long (hundreds-of-My-) intervals, only to rebound at other times, all while destroying via harmonics or Pr any petrified evidence of speciation systematically-periodically. The conclusion that the constant drop is a sign of an underlying resonance is supported by a steady global in-size reduction of polygonal (resonant) geomorphology, such as patterning and cratering. Specifically, such geomorphology has changed from ancient kilometer-scale shapes, primarily polygonal craters (Faraday latticing) mostly hexagonal and seen throughout the Solar system, to present-day metre-scale shapes like patterns in salt deserts; see, e.g., Omerbashich (2020a) and Lasser (2019).

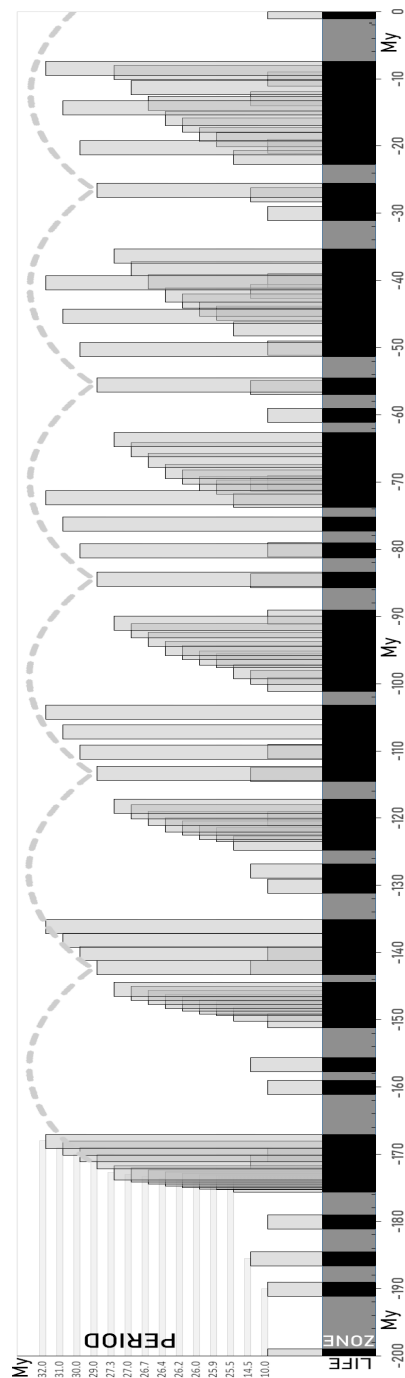


Figure 7. Time-domain-superimposing all claims of periods in mass-extinctions, as compiled by Rampino and Prokoph (2020) (see their Table 1), reveals the virtual impossibility of life on Earth. All periods were used (regardless of statistical significance) due to the inherent inability of Fourier and other classical methods of spectral analysis to correctly estimate the statistical significance of spectral periods (Erlykin et al., 2017, 2018). The plot reveals an impossibility of life on Earth in the Phanerozoic (the last half a billion years). The point of origin selected at -200 My as around the middle of the Phanerozoic. The plot assumes all life originated at an instant or during a short interval (of several My). Bar line: grayness represents life, blackness impossibility of life. Bin spread fixed at 1 My, to represent macroevolutionary bursts (minimum time required for a single evolutionary step to develop adaptively in a species) per Uyeda et al. (2011). The 10-My bin is a gauge best-fitting the overlap intervals, averaging the time for which most species continue after an extinction event (cf. Barnes et al., 2021, who found that most species continue for more than 30 My past an extinction, while many drops in diversity without recovery are not associated with mass extinction events at all). The dashed arc depicts a resonance period (wave) as it rolls out in the time domain. Based on the varying spread in overlapping, the plot rules out galactic cyclic causes to mass extinctions, revealing that life on Earth would be practically impossible if most of the reports alleging periodic mass-extinctions were results of using reliable data and proper preparation and processing techniques. Instead, the precessional resonance via its carriers of destructive angular deflection (such as the 26.5-My Rampino period, Table 3, and lower-order harmonics) causes polarity reversals during TREs while simultaneously decimating strata — including the record of (thus “periodic”) mass extinctions.

Finally, alleged periods of mass-extinctions superimposed in the time-domain reveal that life during Phanerozoic (including today) practically could not exist, or periodic mass-extinctions are not real; see Fig. 7. Note here that the obliquity-induced precessional resonance does not outright discard any possibility of mass extinctions as such, like the Permian–Triassic extinction event. Instead, the record of evolution gets decimated together with, or within a short time from, topography-reshaping TREs. This reasoning agrees with the recent find that most species continue after an extinction event for more than 30 My, while many post-event drops in diversity without recovery are not associated with mass extinction events at all (Barnes et al., 2021). Similarly, pre-Milankovitch views that climate periodicity is due to changes in Earth’s magnetic field (Puetz et al., 2016, Raup, 1985) made sense only due to the geomagnetism record’s dominant bias in the same way. Then geomagnetism polarity reversals, polygonal “cratering”, and “periodic” mass-extinction records describe the same phenomenon of obliquity-triggered precessional mechanical resonance that causes stratigraphically recorded changes — in geomagnetism and cratering primarily. This recording is due to actual resonance waves in the solid matter (Faraday latticing), but only apparent changes in evolution — as evolutionary evidence itself (residing embedded within solid matter) gets exposed to damaging resonance waves. Note here that, while the geomagnetism record gets decimated too, it is the least affected type of solid-matter-residing paleodata since only simultaneous total (rarest) reshaping of entire continents can alter that record significantly in terms of its systematic information contents.

Other examples of GVSA’s ability to compute resonances in data at absolute accuracy and 99% or 95% significance levels include resonance extractions from time-series of $M_w 5.6+$ earthquakes’ occurrences for solid Earth (Omerbashich, 2000b) and from moonquakes for solid Moon (Omerbashich, 2000a), both cases also reporting 89%- and 67%-significant harmonics as well, all the way up to 1/72 of the forcer in the case of solid Earth. Again, that the GVSA can absolutely accurately extract solid-matter resonance as it forms actual particle waves, was shown from continuous GPS data by Omerbashich (2022). Worth noting here is the main difference between detecting orbital resonances transferred directly (mechanically and/or by the way of gravity) into the solid matter as particle waves, and those impressed into gaseous matter indirectly as a temporally undersampled powerless signal: while in the latter case, characteristic of various types of paleodata, statistical fidelity of so extracted resonance periods normally is $\Phi < 12$ and often $\Phi \ll 1$, $\Phi \ll\ll 1$, and on, in the former case it is regularly $\Phi \geq 12$ and often $\Phi \gg 12$, $\Phi \gg\gg 12$, and on. For example, in the extractions reported by *ibid.*, and which dealt with >99% populated time-series, fidelity was found to occupy 12–11 ranges on the shortest, while reaching 60,000–9,000 ranges on the longest periods.

9. Identification of moderation carrier

To show that the Rampino period, P_R , does represent the precessional resonance’s crosscyclic (multi-harmonic) carrier of the peak angular deflection, I examine phase relations of P_R to P . Should such a causal relation exist, it would expose P_R as itself a modulation of the already phase-shifted precession p . In that case, P_R would also be the primary modulation of P , and thereby the only sole actor besides $(2\pi p, P_i)$ resonance in the 1–40 My band.

Since not an orbital period itself, we cannot expect for the P_R to have 2π -phase-shifted, i.e., in the same way as precession and obliquity did. Then, and since P_R was extracted as a sole actor only once — in the absence of (p, P_i) , the way in which P modulates P_R is determined entirely by the effects of annual variation in the equation of time on P itself, Fig. 3. Puetz et al. (2016) have already shown the effect of this variation on P , albeit in the 1 ky–1 My band and for the base cycle in that band, as a phase coefficient $k = 2.829$. (Note that those authors, based on observations of the discrete time translation symmetry

alone (i.e., of paleodata periods tripling, halving, and doubling), mistakenly assigned the unit of a solar year to the above coefficient of proportionality and called it a period, $P_{0,0}$, when in fact it is the symmetry alone which arises due to annual variation in the equation of time, Fig. 3).

Since P_R is tacitly assumed itself affected by the same variation, and we want to test an implied physical hypothesis (of P_R being the strongest resonance period, on a par with P itself, or even stronger in terms of damage potential to solid matter), k is already a phase-shift of P_R and is a (dimensionless) coefficient. Then all we need to do to establish or rule out the implied physical hypothesis is compare the match of P_R and P against k . And since we can see that $P_R / P = 2.838$, the matching is within 3‰, or practically absolute, so the results from the GVSA, Fig. 3, are independently and numerically validated.

Furthermore, since k itself (again, as a coefficient instead of period) is just a reflection of π , i.e., $k = 9/10 \cdot \pi$ to within 0.5‰, i.e., practically $1 \cdot \pi$, this odd-multiple π -phase-shift of P_R from P reveals that P_R is a carrier of classical destructive rather than constructive (even-multiple) interference, itself phase-shifted from P so that $P_R = (9/10) \pi \cdot P$. The instability in the $k = \pi$ equality, as due to a 9/10 reflection alone (itself a reflection to within 0.5‰), is an independent confirmation that the destructive interference of P_R is due to inherently unstable angular deflection of a mechanical resonance.

Thus P_R originates as the system period, i.e., around the mid-band and as a $(9/10) \pi \cdot P$ modification itself — as the result of an interplay of all resonance harmonics, i.e., the above-noted entire train, Fig. 2 and Table 2. This interplay is why P_R , while phase-shifted itself (albeit not by 2π), forces (or relays, rather) its own, higher-order, harmonics, Table 4, revealing its terrestrial rather than galactic or other origins, and P as the resonance driver. Although an excess critical speed and angular deflection make for the potentially destructive side of any mechanical resonance, the most potentially damaging feature of such resonance in the case of closed physical systems like the Earth-Moon-Sun is far more critical. Namely, it brings about the above-mentioned resonance magnification effect via frequency demultiplication, which can magnify energy injected resonantly into a physical system by 100s of times (Omerbashich, 2007a, Den Hartog, 1985). This magnification can then be channeled also through a carrier wave such as P_R .

Such sole-actor, energetic period like P_R can co-instigate geomagnetic polarity reversals and be capable of various other upheavals on and inside the Earth. Those cataclysms include resonant (and therefore mixed, intermittently periodic-quasiperiodic), all-transforming events such as plate tectonics and reformatting continents, which then significantly alter strata too. However, the complete record of geomagnetic polarity reversals is not periodic with P_R . This apparent absence is due to the varying ability (to complete inability) of the incessant resonance train's member waves to move across vast distances and depths. These individual harmonics separately also partake during TREs in decimating of strata and other records of paleodata, thus adding an appearance of pseudoperiodicity or chaos in data. The variation in an individual harmonic's abilities to move as a wave depends upon which resonance frequency turns into the largest destroyer-wave feeder at a given time and location. Identifying and ignoring (turning on and off) those waves in all combinations can then help map the underlying dynamics in space and time. The significant alteration of strata by a P_R wave during TREs, and then the downward continuation of that wave and its harmonics, and then penetrating and finally enveloping the inner core, is the core/polarity reversal mechanism.

Numerous models support the results of this study in some of its aspects. For instance, the Pétrélis et al. (2011) model supports the possibility that such a mechanism is at play by establishing a link between plate tectonics and reversal frequency, i.e., a correlation between lopsided continental geomorphology and the soon-following reversals. While corroborating the Carbone et al. (2006) find of reversals clustering, a model by Stefani et al. (2007) exhibited a good agreement with the CKGPTS95 and identified resonant features in geomagnetic polarity reversals. On the other hand, while unable to confirm the clustering, a core-rotation model by Hoyng and Duistermaat (2004) has suggested

that polarity reversals are relatively fast events. In addition to numerical and analytical modeling, numerous experiments also addressed the geomagnetic reversals problem. Thus, dynamos generated by mechanical driving such as precession or tidal forcing have become popular in recent years, and experiments focusing on precession-driven flows were conducted in various labs (Giesecke et al., 2019).

The high accuracy and precision of computations of previously reported periodicity, besides owing advantage to the GVSA, also mean that virtually all $\sim 3P$ periodicity previously reported from paleodata most likely are underestimated and overestimated extractions of P_R , as evading detection is one of the characteristics of resonance carrier waves. Besides, while indeed detecting a $\sim 3P$ period in paleodata, many of such reports also found no statistical significance in it (Table 1 of Rampino and Prokoph, 2020), and variable significance is another characteristic of resonance carrier waves (in addition to being characteristic of using inapt computational tools and approaches, as described above).

As extracted in this study, P_R is matched practically exactly by the average from all the estimates of dominant periods from the extinction record. However, the cratering record's average is significantly mismatched (*ibid.*). This difference was as expected since encapsulated or sheltered strata preserve histories of natural disasters more faithfully than the craters exposed to weather and erosion ever could. Previous reports corroborate the find of P_R in geomagnetic reversals of this study, e.g., by Raup (1985), who, in a coarse study, found geomagnetic reversals periodic at 30 My, which probably was an overestimated P_R .

10. Discussion

Modern approaches to dating events and fossils in the geological record over the past forty years have relied heavily on tuning that record to repeatable astronomical events in the Solar system — especially so for missing ends of strata series or otherwise obscured parts such as most of paleodata older than ~ 40 My. But as with any modeling, this contrived “clockwork geoscheme” is only as good as the awareness of end-users of all its drawbacks and potential error sources. It took only a few decades for ad-hoc tying arbitrarily selected portions and ranges of the record to celestial mechanics to diverge into the realm of spectral analyses of so tuned datasets declaring practically every adynamical reflection of astronomical cycles as verification of some genuinely natural process. Spectral analyses of diversity in paleodata, for example, often invoke even extraterrestrial causal mechanisms, such as galactic or universal, as the cause of mass extinctions — thereby implied as repeating themselves. However, such explanations are not convincing since they do not explain the appearance of equally justifiable and possibly related sub-harmonics in the spectral analysis (Baker and Flood, 2015). Not only that extraterrestrial causes need not be invoked to explain widely present periodicity in paleodata, but those periods themselves as extracted are also suspect due to undersampling and overestimating issues pervading analyses of the geological record. For example, as seen in Fig. 7, periods of so-called periodic mass extinctions superimposed in the time domain make most of life on Earth seem virtually impossible.

By focusing on the rarely probed 1–40-My long band, it was possible to avoid mathematically the dominance of the axial, p , and apsidal, p_1 , precessions, Fig. 1 — amplified and focused in the process of astronomical tuning of the CKGPTS95 timescale of geomagnetic reversals. This band has revealed an annually-secularly modulated precession, $P = 9.34737$ My, along with its entire ensemble of harmonics $P_i = P/i$, $i = 1\dots 9$; $i \in \mathbb{Z}^+$, Fig. 2. The $P = P_1 = 360^\circ \cdot p$ is the lead (annual) modulation of precession harmonics due to annual variations in the equation of time, Fig. 3. Rather than cumbersomely comparing individual peaks in the timescale spectrum to discern the possible modulation impressor or trigger, computing the spectrum of that timescale calibration's spectrum in the same band reveals

the obliquity's annual modulation $P' = 3.56977$ My = $360^\circ \cdot \frac{1}{4}p' = 9.916$ ky, or the obliquity's base cycle $\frac{1}{4}p'_{\text{theor}} = 41000/4$ to within 3%, then overlies the entire record and triggers the here extracted precessional resonance.

Hence, when spectrally analysing paleodata, it is not sufficient to declare a statistically significant period also physically significant or outright discard an extracted period that is statistically insignificant. Such detections warrant further investigation into possible mutual mathematical relationships among statistically significant periods. If a detected period is part of a modulation ensemble, i.e., one of (usually many) mutually mathematically directly related periods, then such a batch represents n -reflections (integer multiples of the shortest period – the driver) or harmonics (integer splits of the longest period – the forcer) or unspecified modulations (ratios of the driver or the forcer). Reflections also can appear as forcers of other modulations, which are then also termed reflections and not harmonics as the term harmonic is reserved for possibly dynamical (relatively high-energy) cyclic physical phenomena. If the driver or forcer turns out to be astronomical – like the Earth's axial precession period, of ~26 ky – then its entire ensemble of modulations is physically insignificant or meaningless, too. Only after enforcing of entire such ensemble (where it suffices to ignore just the driver or forcer for its entire ensemble to get ignored too) can one begin a quest for periods as signatures of natural forces or phenomena that had dynamically affected the data examined.

Then additional criteria to determine the physical meaningfulness of statistically significant periods are required. As mentioned earlier, one such criterion is the (statistical) fidelity, Φ : usually, periods with $\Phi \geq 12$ reflect some dynamical process that acted upon the data sampled. Physical constraints also could be invoked. For example, since we know that life on Earth does not die out every precession cycle, the precession alone most likely is not a mass-extinction driver. Likewise, we know that the Earth magnetic poles do not revert (the geomagnetic field does not change polarity) every precession either, so the precession alone most likely is not a polar-reversals forcer; and so on. These physical constraints say nothing about precessional resonances since the latter include numerous mechanical waves of varying energy levels and destruction potential.

Thus the Earth axial precession's modulation due to annual variation in the equation of time (Fig. 3), $P = 9.34737$ My, has been reported previously as a genuine and statistically significant spectral peak. In one of more extreme examples of confusing means and ends, Martinez and Dera (2015), while aware that “grand orbital cycles” (on the order of My) are just modulations of astronomical cycles, nevertheless declare a ~9-My peak they found in the Jurassic–Early Cretaceous carbon cycle also physically significant. They even proclaim it “an important metronome of the greenhouse climate dynamics” – all based on statistics alone.

Other workers, however, do recognize this modulation as physically unrealistic and proceed on to examine possible non-orbital causes for its presence, see, e.g., Boulila et al. (2012) study of a ~9-My pseudoperiod in Cenozoic carbon isotope record $\delta^{13}\text{C}$ but who also fail to explain the presence of this pseudoperiod. In an assessment of a recent example from non-marine tetrapod extinction record (compiled by Rampino et al., 2020) insensitive to the ocean-tidal component as the largest systematic noise constituent, Omerbashich (2021) found that most if not all of the periods claimed in the past as mass-extinction cycles are instead astronomical reflections, of Earth's axial precession primarily, i.e., $n \cdot p$. A mass-extinction period of 27.5 My extracted using circular and Fourier methods from their compilation and cratering by Rampino and Caldeira (2015), was previously questioned by Meier and Holm-Alwmark (2017) over circular method use and then by Omerbashich (2021) over Fourier method use. As mentioned, *ibid.* showed that the 27.5-My period is just a ~3P modulation (the above-discussed tripling in rigid multi-body resonances; see, e.g., Prokoph and Puetz, 2015). Previously, Omerbashich (2006, 2007b) had demonstrated on a flawed report by Rohde and Muller (2005) that data manipulations and inapt techniques such as the Fourier class of spectral analysis techniques can result in a detection of apparently significant periods in marine diversity data as well.

Since P is controlled by the Earth's own orbital (annual) cycle primarily, subsequently driven into secular, centennial, millennial modulations, and on — the total modulation of P extends *ad infinitum*. Thus, the results of this study are precession rate-independent and readily applicable to any geological interval to Triassic, thanks to the strict nature of paleomagnetism primarily (Berger, 2012), but also beyond, since the main find is strictly astronomical in origin. For example, the $10P$ and $100P/7$ reflections were first reported by Omerbashich (2006) from the Sepkoski fossils record as 91.3-My and 140.23-My at the 99%-significance level. The former of the two periods was confirmed by Boulila et al. (2018), who also report a ~9.3-My cyclicity as previously attributed to the long-period Milankovitch band based on the Cenozoic record, as well as a ~250-My megacycle which they attributed even to tectonic causal mechanisms but which too is just an annually-secularly induced reflection, $100P/4$, Fig. 3. The reason for the latter period to be so persistent (very long) is in it being a crosscycle — amplified and maintained by the $70P'$ reflection as well, Fig. 5.

Other reports of reflections, sensationalized as key or justified by cryptic galactic causes, fill the literature and are often picked by national and international media in search of a sensation more. In one of the most notorious such examples, Boulila (2019) reported “prominent ~9 and ~36 My” cyclicities in Cenozoic–Cretaceous benthic foraminifera $\delta^{18}\text{O}$, but a look at Fig. 3 tells that those are just annually-secularly induced P and its $\sim 4P$ reflection, respectively. The only reason the often reported ~36-My period appears so persistent and omnipresent across the geological record is that it too is a crosscycle — amplified by $10P'$ reflection, Fig. 5, as well as the 2π (circular) modulation $360^\circ \cdot p''$, where p'' is the Earth eccentricity astronomical period, of ~100 ky.

More of the similarly simple mathematical relations are noticed readily among detected periods in paleodata. For example, looking at the nine periods from Table 2 of Omerbashich (2021), the 33.84146-My period is just the 8.48624-My period quadrupled, or 6.67870-My quintupled, while the 11.93548-My period is simply the 7.95129-My period tripled-halved, etc. As mentioned earlier, these subharmonic relations — doubling, halving, and tripling primarily — represent discrete time translation symmetry characteristic of subharmonic resonant response of rigid multi-body systems to external periodic forcing. For instance, the above-discussed ~3P periods often are reported in the literature, but such reports mostly used inapt techniques that cannot distinguish resonances from resonance drivers.

The type of result obtained in the present study calls for an addition to the Milankovitch theory (see, e.g., Berger, 2012) to differentiate among varying power of the Milankovitch — as demonstrated here — resonant, cycles. This varying power from one to another resonance wave explains the 100-ky cyclicity problem of that theory — the otherwise inexplicable termination events when astronomical cycles (and, in the sense of resonance theory, their reflections or harmonics) switch in the role of planetary change driver. The latest such recorded event of glacial-interglacial switching, the Mid-Pleistocene Transition, had occurred ~1 My ago. At that time, the ~40-ky period gave in to the ~100-ky period (Bajo et al., 2020). This event resembles an energy-transfer event across frequencies — the relatively brief period of nonlinear resonance (Rial et al., 2013). The difficulties in assigning physical mechanisms to generate the necessary gain to power the 100 ky cycles led Liu (1992) to examine frequency resonance phenomena among the orbital parameters as an alternative source for the transition, and he concluded that it is the Earth obliquity which modulates a major 100 ky periodicity (Hinnov, 2000). As shown earlier, and supporting that result, the Mid-Pleistocene switch from the obliquity's p' period to a 100-ky period was not a transition from obliquity to eccentricity as the Earth's dominant climatic driver, but an obliquity-triggered resonant jump from one to another resonant frequency coincidentally near the duration of one eccentricity cycle. The orbitally triggered (and obliquity-triggered too) precessional resonance is the most reasonable physics-based, all-explanatory addition to the intellectually already pleasing Milankovitch theory.

The addition to the Milankovitch theory is overdue, so to recognize that that theory is just a special case of the far more complex Earth–Moon–Sun (or rather obliquity–precession–Earth) resonant energy transfer. Similarly, that theory’s spatiotemporal domain extends only for as long as a specialized energy band (currently determined by one of the tailing harmonics of the precessional resonance) of the resonant-dynamic energy band that at present envelopes and shapes our planet lasts before it dissipates. As it dissipates, it does it only so to make room for another precessional-resonant energy band belonging to another resonance harmonic (and so on, until P_R), and which will be describable by some other form of the Milankovitch theory — not entirely unlike the current one. The energy supplied thus to the Earth is globally cumulative since the Earth acquired the Moon ~ 4450 billion years ago, and thus the only known mechanism for a growing Earth proposed by many, e.g., Schmidt and Embleton (1981) and Maxlow (2021). Omerbashich (2020a) proposed that one of Mars’s moons be reassigned to the Earth to create interference before the Earth reaches the state of energy overload and implodes.

The present study revealed that the concept of time crystal known from quantum physics is also macroscopic. This synchronization of quantum type in vibrations of dynamic structures at interplanetary and interstellar scales could arise tidally due to a satellite galaxy or universe. In the first attempt to link the Milankovitch theory to Earth’s internal processes at Myr time scales, Boulila et al. (2021) erroneously speculated that the most likely phenomenon linking insolation-climate with the Earth’s internal processes lies in climatically-resonantly driven mass changes on Earth surface, such as imagined sea level variations due to climate change. In their opinion, the potential link between external and internal processes would thus manifest as interaction and feedback rather than a direct orbital forcing of the solid Earth. However, as I showed in the present study computationally and confirmed by exposing Earth’s behavior as that of a gigantic macroscopic time crystal, the exact opposite holds: a direct orbital forcing of the solid Earth, her interior, and the Milankovitch process has been taking place in unison since time immemorial. This cross-scale-verified computational discovery conclusively confirms the genuine nature of the South Atlantic Anomaly of the geomagnetic field low as a precursor of an upcoming reversal, contrary to recent speculations, e.g., by Nilsson and Muscheler (2022).

11. Conclusions

Discrete time translation symmetry (seen commonly in paleodata as period multiplication and halving), 2π -phase-shifts, and $\frac{1}{4}$ -lockstep to the forcer — previously thought to arise together only in a subharmonic response of a time crystal to external periodic forcing and to be confined to quantum scales — characterize the here reported global geophysical detection of the mechanism for geomagnetic polarity reversals from the CKGPTS95 timescale calibration, as arguably the best record of paleodata available for this type of studies. This macroscopic confirmation of fundamental properties of the discrete time crystal concept known from quantum physics means it is unremarkable while revealing the scale-invariant nature of physics from a previously unknown, planetary geodetic perspective. This result has fundamental implications as it relates macroscopic with quantum physics: *the (planetary) time crystal is formed by the many-body entrainment causing precession resonance that, in turn, moderates (geo)magnetic polarity.* In quantum dynamics, such particle entrainment can take the form of collisions, causing Feshbach resonances.

This fundamental property was arrived at by analyzing paleodata periods previously claimed in the literature as standalone-significant cyclicity (indicative of a dynamical process) but which turned out to be just multiples or fractions of some other periods that appear as periods in extinctions and other geological records. Thus previously claimed very long periods in paleodata, such as the ~ 9 -My, are modulations primarily of the Earth axial precession. Together with respective modulations (reflections and harmonics), they arise resonantly under the obliquity and other triggers such as varying crustal thickness,

mantle flows, and inner-core dynamics — basically any obstacles in the path of macroscopic Faraday instabilities. Future analyses of non-astronomical periodicity in paleodata must enforce (mathematically ignore) precession periods and their annual 2π -phase-shifted modulations and entire precessional resonance ensembles, depending upon the band or scale of extraction. It should become a standard procedure to mathematically make the said astronomical periods and their modulations vanish from spectra before drawing conclusions on causality and physical mechanisms that affect dynamical processes at all scales on Earth, from quantum to planetary.

The global approach to treating the currently accepted CKGPTS95 timescale (calibration) of geomagnetic polarity reversals, viewed as the gauge for analyzing planetary paleodynamics, has confirmed the generally accepted absence of lonesome (including extraterrestrial) mechanisms for periodic polarity reversals. At the same time, that approach enabled deducing the 0.02–40-My-bands resonance as it uses its inherent 26.5-My Rampino period for a carrier of cumulative resonant destruction of obstacles in the resonance's path. As the orbital energy transfer had already occurred in those mechanical resonances, they become in their low-frequency part transformatively destructive and plate tectonics-catalyzing; the energy transfer constitutes an energy injecting mechanism for the astronomical forcing of climate to work, albeit in ways previously unseen. Namely, the 2π -phase-shifted precessional resonance extracted in the 1–40 My band is also the scale-invariant energy-transfer mechanism of the Milankovitch theory as now just a special case applicable to the current stage of the Earth-Moon-Sun resonant dynamics. Thus sedimentary stratigraphy keeps a record of this orbital-to-mechanical resonant energy transfer so that long-period (My-) scales of resonant periodicity no longer require a major extraterrestrial (galactic) or tectonic driver to explain changes in paleodata. Instead, the precessional resonance at its wave cycles, during rare but cataclysmic Transformative Resonant Events (TREs) characterized by general destruction due to combined effects of interference and angular deflection of its most energetic parts via the 26.5-My Rampino carrier wave, downward penetrates the inner core, envelopes it, and mechanically flips the geomagnetic polarity and cores. In doing so, while modifying all solids, including the crust, it also decimates the geological record with the evidence of evolution, creating the false record of periodic mass extinctions that instead records precession-induced terraforming events. Over geological history, the (incessant) resonance has caused geomagnetic polarity excursions while masking sudden cataclysms under what today appears like gradual processes. Other geophysical theories dismissed in the past over their lack of mechanism are now more plausible, such as that on expanding Earth.

A pivotal question that needs to be addressed by future research then is if the upcoming geomagnetic polarity flip will be just an excursion or a complete reversal. In the latter case, an accompanying TRE is certain. Given thousands of harmonics in-between consecutive P_R (besides the millions of puny reflections accumulated via repetitive annual imprinting that creates a projector effect), architecture and urbanism in futuristic concepts generally must ensure the survival of life until successful space colonization, as sheltered and confined until then to underlake and undersea super-protective habitats independent of topography.

Acknowledgments: The spectra were computed using the least-squares spectral analysis scientific software LSSA v.5.0, based on the rigorous method by Vaníček (1969, 1971), now available in an open-source version from <http://www2.unb.ca/gge/Research/GRL/LSSA/sourceCode.html>.

Declaration of interest: The author declares no conflict of interest.

Data Access Statement: All data generated or analyzed during this study are included in this article.

References

Bailer-Jones, C.A.L., 2009. The evidence for & against astronomical impacts on climate change & mass extinctions: a review. *Int. J. Astrobiol.* 8, 213–219. <https://doi.org/10.1017/S147355040999005X>

Bajo, P., Drysdale, R.N., Woodhead, J.D., Hellstrom, J.C., Hodell, D., Ferretti, P., Voelker, A.H.L., Zanchetta, G., Rodrigues, T., Wolff, E., Tyler, J., Frisia, S., Spotl, C., Fallick, A.E., 2020. Persistent influence of obliquity on ice age terminations since the Middle Pleistocene transition. *Science* 3676483, 1235–1239. <https://doi.org/10.1126/science.aaw1114>

Baker, R.G., Flood, P.G., 2015. The Sun–Earth connect 3: lessons from the periodicities of deep time influencing sea-level change and marine extinctions in the geological record. *SpringerPlus* 4, 285. <https://doi.org/10.1186/s40064-015-0942-6>

Barnes, B.D., Sclafani, J.A., Zaffos, A., 2021. Dead clades walking are a pervasive macroevolutionary pattern. *Proc. Natl. Acad. Sci. U.S.A.* 11815, e2019208118. <https://doi.org/10.1073/pnas.2019208118>

Bassinot, F.C., Labeyrie, L.D., Vincent, E., Quidelleur, X., Shackleton, N.J., Lancelot, Y., 1994. The astronomical theory of climate and the age of the Brunhes-Matuyama magnetic reversal. *Earth Planet. Sci. Lett.* 1261–3., 91–108. <https://doi.org/10.1016/0012-821X94.90244-5>

Berger, W.H., 2012. *Milankovitch Theory - Hits and Misses*. Milutin Milankovitch Medal Lecture at the EGU General Assembly, 22–27 April, Vienna, Austria. Retrieved from UC San Diego: Library – Scripps Digital Collection, <https://escholarship.org/uc/item/95m6h5b9>

Boulila, S., Haq, B.U., Hara, N., Müller, R.D., Galbrun, B., Charbonnier, G., 2021. Potential encoding of coupling between Milankovitch forcing and Earth's interior processes in the Phanerozoic eustatic sea-level record. *Earth Sci. Rev.* 220:103727. <https://doi.org/10.1016/j.earscirev.2021.103727>

Boulila, S., 2019. Coupling between Grand cycles and Events in Earth's climate during the past 115 million years. *Sci. Rep.* 9, 327. <https://doi.org/10.1038/s41598-018-36509-7>

Boulila, S., Laskar, J., Haq, B.U., Galbrun, B., Hara, N., 2018. Long-term cyclicities in Phanerozoic sea-level sedimentary record and their potential drivers. *Global Planet. Change* 165, 128–136. <https://doi.org/10.1016/j.gloplacha.2018.03.004>

Boulila, S., Galbrun, B., Laskar, J., Palike, H., 2012. A ~9myr cycle in Cenozoic δ13C record and long-term orbital eccentricity modulation: Is there a link? *Earth Planet. Sci. Lett.* 317–318, 273–281. <https://doi.org/10.1016/j.epsl.2011.11.017>

Boulila, S., Galbrun, B., Miller, K.G., Pekar, S.F., Browning, J.V., Laskar, J., Wright, J.D., 2011. On the origin of Cenozoic and Mesozoic "third-order" eustatic sequences. *Earth-Sci. Rev.* 109, 94–112. <https://doi.org/10.1016/j.earscirev.2011.09.003>

Cande, S.C., Kent, D.V., 1995. Revised calibration of the geomagnetic polarity timescale for the Late Cretaceous and Cenozoic. *J. Geophys. Res.* 100B4, 6093–6095. <https://doi.org/10.1029/94JB03098>

Cande, S.C., Kent, D.V., 1992. A new geomagnetic polarity time scale for the Late Cretaceous and Cenozoic. *J. Geophys. Res.* 97B10, 13917–13951. <https://doi.org/10.1029/92JB01202>

Carbone, V., Sorriso-Valvo, L., Vecchio, A., Lepreti, F., Veltri, P., Harabaglia, P., Guerra, I., 2006. Clustering of polarity reversals of the geomagnetic field. *Phys. Rev. Lett.* Mar 31. 9612, 128501. PMID: 16605965. <https://doi.org/10.1103/PhysRevLett.96.128501>

Chang, H.-Y., Moon, H.-K., 2005. Time-series analysis of terrestrial impact crater records. *Publ. Astron. Soc. Jpn.* 573, 487–495. <https://doi.org/10.1093/pasj/57.3.487>

Craymer, M.R., 1998. *The Least Squares Spectrum, Its Inverse Transform and Autocorrelation Function: Theory and Some Applications in Geodesy*. Ph.D. Dissertation, University of Toronto, Canada. URI: <https://hdl.handle.net/1807/12263>

De Santis, A., Qamili, E., Cianchini, G., 2011. Ergodicity of the recent geomagnetic field. *Phys. Earth Planet. Inter.* 1863–4., 103–110. <https://doi.org/10.1016/j.pepi.2011.04.008>

Den Hartog, J.P., 1985. *Mechanical Vibrations*. Dover Publications, New York, United States. ISBN 0486647854

Emiliani, C., 1955. Pleistocene Temperatures. *J. Geol.* 636, 538–578. <https://doi.org/10.1086/626295>

Erlykin, A.D., Harper, D.A.T., Sloan, T., Wolfendale, A.W., 2017. Mass extinctions over the last 500 myr: an astronomical cause? *Palaeontology* 60, 159–167. <https://doi.org/10.1111/pala.12283>

Erlykin, A.D., Harper, D.A.T., Sloan, T., Wolfendale, A.W., 2018. Periodicity in extinction rates. *Palaeontology* 61, 149–158. <https://doi.org/10.1111/pala.12334>

Feng, F., Bailer-Jones, C.A.L., 2015. Obliquity and precession as pacemakers of Pleistocene deglaciations. *Quat. Sci. Rev.* 122, 166–179. <https://doi.org/10.1016/j.quascirev.2015.05.006>

Giesecke, A., Vogt, T., Gundrum, T., Stefani, F., 2019. Kinematic dynamo action of a precession-driven flow based on the results of water experiments and hydrodynamic simulations. *Geophys. Astrophys. Fluid Dyn.* 1131-2., 235–255. <https://doi.org/10.1080/03091929.2018.1506774>

Gradstein, F.M., Ogg, J.G., Smith, A.G., Bleeker, W., Lourens, L.J., 2004. A new Geologic Time Scale, with special reference to Precambrian and Neogene. Contains parts of the Geologic Time Scale 2004. *Episodes* 272, 83–100. <https://doi.org/10.18814/epiugs/2004/v27i2/002>

Grippo, A., Fischer, A.G., Hinnov, L.A., Herbert, T.D., Premoli Silva, I., 2004. *Cyclostratigraphy and chronology of the Albian stage Piobbico core, Italy*. In: D'Argenio, B., Fischer, A.G., Premoli Silva, I., Weissert, H., Ferri, V. (Eds.). *Cyclostratigraphy: Approaches and Case Histories*. Society for Sedimentary Geology Special Publication 81, 57–81. <https://doi.org/10.2110/pec.04.81.0057>

Guo, L., Marthaler, M., Schön, G., 2013. Phase Space Crystals: A New Way to Create a Quasienergy Band Structure. *Phys. Rev. Lett.* 111, 205303. <https://doi.org/10.1103/PhysRevLett.111.205303>

Hays, J.D., Imbrie, J., Shackleton, N.J., 1976. Variations in the Earth's orbit: Pacemaker of the Ice Ages. *Science* 194, 1121–1132. <https://doi.org/10.1126/science.194.4270.1121>

Hilgen, F.J., 1991. Extension of the astronomically calibrated polarity: time scale to the Miocene/Pliocene boundary. *Earth Planet. Sci. Lett.* 1072, 349–368. [https://doi.org/10.1016/0012-821X\(91\)90082-S](https://doi.org/10.1016/0012-821X(91)90082-S)

Hinnov, L.A., 2013. Cyclostratigraphy and its revolutionizing applications in the Earth and planetary sciences. *GSA Bulletin* 12511–12., 1703–1734. <https://doi.org/10.1130/B30934.1>

Hinnov, L.A., 2000. New Perspectives on Orbitally Forced Stratigraphy. *Annu. Rev. Earth Planet. Sci.* 281, 419–475. <https://doi.org/10.1146/annurev.earth.28.1.419>

Hinnov, L.A., Ogg, J.G., 2007. Cyclostratigraphy and the astronomical time scale. *Stratigraphy* 42–3., 239–251

Hoyng, P., Duistermaat, J.J., 2004. Geomagnetic reversals and the stochastic exit problem. *Europhys. Lett.* 682, 177–183. <https://doi.org/10.1209/epl/i2004-10243-1>

Huang, C., Hinnov, L.A., Fischer, A.G., Grippo, A., Herbert, T., 2010. Astronomical tuning of the Aptian stage from Italian reference sections. *Geology* 38, 899–902. <https://doi.org/10.1130/G31177.1>

Ikeda, M., Tada, R., 2013. Long period astronomical cycles from the Triassic to Jurassic bedded chert sequence Inuyama, Japan: geologic evidences for the chaotic behavior of solar planets, *Earth Planets Space* 65, 351–360. <https://doi.org/10.5047/eps.2012.09.004>

Ikeda, M., Tada, R., Sakuma, H., 2010. Astronomical cycle origin of bedded chert; middle Triassic bedded chert sequence, Inuyama, Japan. *Earth Planet. Sci. Lett.* 297, 369–378. <https://doi.org/10.1016/j.epsl.2010.06.027>

IUGS, 1967. A comparative table of recently published geological time-scales for the Phanerozoic time-explanatory notice. International Union of Geological Sciences – Commission on Geochronology for coordination of radiometric and stratigraphic data in the development of a world time-scale. *Nor. J. Geol.* 474, 375–380

Kinkhabwala, A., 2013. *Maximum Fidelity*. Max Planck Institute of Molecular Physiology report. arXiv, <https://doi.org/10.48550/arXiv.1301.5186>

Lasser, J., 2019. *Geophysical Pattern Formation of Salt Playa*. Ph.D. dissertation, Division of Mathematics and Natural Sciences, University of Gottingen, Germany, pp. 200. <http://hdl.handle.net/11858/00-1735-0000-002E-E5DB-2>

Liu, H.S., 1992. Frequency variations of the Earth's obliquity and the 100-kyr ice-age cycles. *Nature* 358, 397–399. <https://doi.org/10.1038/358397a0>

Lutz, T., 1985. The magnetic reversal record is not periodic. *Nature* 317, 404–407. <https://doi.org/10.1038/317404a0>

Martinez, M., Dera, G., 2015. Grand astronomical cycles and their consequences. *Proc. Natl. Acad. Sci. U.S.A.* 11241, 12604–12609. <https://doi.org/10.1073/pnas.1419946112>

Maxlow, J., 2021. *Beyond Plate Tectonics*. Terrella Press, 452 pp. ISBN 9780992565213

Meier, M.M.M., Holm-Alwmark, S., 2017. A tale of clusters: no resolvable periodicity in the terrestrial impact cratering record. *Mon. Not. R. Astron. Soc.* 4673, 2545–2551. <https://doi.org/10.1093/mnras/stx211>

Milankovitch, M., 1941. *Canon of Insolation and the Ice-age Problem*. Königlich Serbische Akademie. Reprint. Zavod za udžbenike i nastavna sredstva, Belgrade, 1998, pp.634. ISBN 8617066199

Miller, K.G., Kominz, M.A., Browning, J.V., Wright, J.D., Mountain, G.S., Katz, M.E., Sugarman, P.J., Cramer, B.S., Christie-Blick, N., Pekar, S., 2005. The Phanerozoic record of global sea level change. *Science* 310, 1293–1298. <https://doi.org/10.1126/science.1116412>

Naish, T., Powell, R., Levy, R. et al., 2009. Obliquity-paced Pliocene West Antarctic ice sheet oscillations. *Nature* 458, 322–328. <https://doi.org/10.1038/nature07867>

Newman, M.E.J., Sibani, P., 1999. Extinction, diversity and survivorship of taxa in the fossil record. *Proc. R. Soc. Lond. B.* 266, 1593–1599. <https://doi.org/10.1098/rspb.1999.0820>

Nickolaenko, A.P., Hayakawa, M., 2002. *Resonances in the Earth-Ionosphere Cavity*. Modern Approaches in Geophysics 19, ISSN 0924-6096. Springer Science & Business Media. ISBN 140200754X, pp.380

Nilsson, A., Muscheler, R., 2022. Recurrent ancient geomagnetic field anomalies shed light on future evolution of the South Atlantic Anomaly. *Proc. Natl. Acad. Sci. U.S.A.* 119(24)e2200749119. <https://doi.org/10.1073/pnas.2200749119>

Olsen, P.E., 2010. *Fossil Great Lakes of the Newark Supergroup—30 years later*. In: Benimoff, A.I. Ed. 83rd Annual Meeting Field Trip Guidebook, New York. New York State Geological Association, College of Staten Island, p. 101–162

Olsen, P.E., 1986. A 40-Million-Year Lake Record of Early Mesozoic Orbital Climatic Forcing. *Science* 2344778, 842–848. <https://doi.org/10.1126/science.234.4778.842>

Olsen, P.E., Kent, D.V., 1999. Long-period Milankovitch cycles from the Late Triassic and Early Jurassic of eastern North America and their implications for the calibration of the Early Mesozoic time-scale and the long-term behaviour of the planets. *Phil. Trans. R. Soc. A.* 3571761–1786. <https://doi.org/10.1098/rsta.1999.0400>

Omerbashich, M., 2022. Detection and mapping of Earth body resonances with continuous GPS. *J. Geophys.* 641, 12-33. <https://n2t.net/88439/x073994>

Omerbashich, M., 2021. Non-marine tetrapod extinctions solve extinction periodicity mystery. *Hist. Biol.* 341, 188-191. <https://doi.org/10.1080/08912963.2021.1907367>

Omerbashich, M., 2020a. Moon body resonance. *J. Geophys.* 63, 30–42. <https://n2t.net/88439/x034508>

Omerbashich, M., 2020b. Earth body resonance. *J. Geophys.* 63, 15–29. <https://n2t.net/88439/x020219>

Omerbashich, M., 2007a. Magnification of mantle resonance as a cause of tectonics. *Geod. Acta* 206, 369–383. <https://doi.org/10.3166/ga.20.369-383>

Omerbashich, M., 2007b. Erratum due to journal error. *Comp. Sci. Eng.* 94, 5–6. <https://doi.org/10.1109/MCSE.2007.79>; full text, <https://arxiv.org/abs/math-ph/0608014>

Omerbashich, M., 2006. Gauss–Vaníček Spectral Analysis of the Sepkoski Compendium: No New Life Cycles. *Comp. Sci. Eng.* 84, 26–30. <https://doi.org/10.1109/MCSE.2006.68>

Omerbashich, M., 2003. *Earth-Model Discrimination Method*. Ph.D. Dissertation, University of New Brunswick, Canada, pp.129. Library and Archives Canada & ProQuest, ISBN 9780494068793. <https://doi.org/10.6084/m9.figshare.12847304.v1>

Pagiatakis, S., 1999. Stochastic significance of peaks in the least-squares spectrum. *J. Geod.* 73, 67–78. <https://doi.org/10.1007/s001900050220>

Pétrélis, F., Besse, J., Valet, J.-P., 2011. Plate tectonics may control geomagnetic reversal frequency. *Geophys. Res. Lett.* 38, L19303. <https://doi.org/10.1029/2011GL048784>

Press, W.H., Teukolsky, S.A., Vetterling, W.T., Flannery, B.P., 2007. *Numerical Recipes: The Art of Scientific Computing* 3rd Ed., Cambridge University Press, United Kingdom. ISBN 9780521880688

Prokoph, A., Puetz, S.J., 2015. Period-tripling and fractal features in multi-billion year geological records. *Math. Geosci.* 47, 501–520. <https://doi.org/10.1007/s11004-015-9593-y>

Puetz, S.J., Prokoph, A., Borchardt, G., 2016. Evaluating alternatives to the Milankovitch theory. *J. Statist. Plann. Inference* 170, 158–165. <https://doi.org/10.1016/j.jspi.2015.10.006>

Puetz, S.J., Prokoph, A., Borchardt, G., Mason, E.W., 2014. Evidence of synchronous, decadal to billion year cycles in geological, genetic, and astronomical events. *Chaos Solitons Fractals* 62–63, Pages 55–75. <https://doi.org/10.1016/j.chaos.2014.04.001>

Rampino, M.R., Caldeira, K., Zhu, Y., 2021. A pulse of the Earth: A 27.5-Myr underlying cycle in coordinated geological events over the last 260 Myr. *Geosci. Frontiers* 126, 101245. <https://doi.org/10.1016/j.gsf.2021.101245>

Rampino, M.R., Caldeira, K., Zhu, Y., 2020. A 27.5-Myr underlying periodicity detected in extinction episodes of non-marine tetrapods, *Hist. Biol.* <https://doi.org/10.1080/08912963.2020.1849178>

Rampino, M.R., Prokoph, A., 2020. Are Impact Craters and Extinction Episodes Periodic? Implications for Planetary Science and Astrobiology. *Astrobiol.* 209, 1097–1108. <https://doi.org/10.1089/ast.2019.2043>

Rampino, M.R., Caldeira, K., 2015. Periodic impact cratering and extinction events over the last 260 million years. *Mon. Not. R. Astron. Soc.* 4544, 3480–3484. <https://doi.org/10.1093/mnras/stv2088>

Raup, D., 1985. Magnetic reversals and mass extinctions. *Nature* 314, 341–343. <https://doi.org/10.1038/314341a0>

Raup, D.M., Sepkoski, Jr., J.J., 1984. Periodicity of extinctions in the geologic past. *Proc. Natl. Acad. Sci. U.S.A.* 813, 801–805. <https://doi.org/10.1073/pnas.81.3.801>

Rial, J., Oh, J., Reischmann, E., 2013. Synchronization of the climate system to eccentricity forcing and the 100,000-year problem. *Nat. Geosci.* 6, 289–293. <https://doi.org/10.1038/ngeo1756>

Rohde, R., Muller, R., 2005. Cycles in fossil diversity. *Nature* 434, 208–210. <https://doi.org/10.1038/nature03339>

Schmidt, P., Embleton, B., 1981. A geotectonic paradox: Has the Earth expanded? *J. Geophys.* 49(1):20–25. <https://n2t.net/ark:/88439/y034403>

Seidelmann, P., 1992. *Explanatory Supplement to the Astronomical Almanac. A revision to the Explanatory Supplement to the Astronomical Ephemeris and the American Ephemeris and Nautical Almanac*. University Science Books, Mill Valley, CA, United States. ISBN 0935702687

Shackleton, N., Berger, A., Peltier, W., 1990. An alternative astronomical calibration of the lower Pleistocene timescale based on ODP Site 677. *Earth Environ. Sci. Trans. R. Soc. Edinb.* 814, 251–261. <http://doi.org/10.1017/S0263593300020782>

Shannon, C.E., 1948. A Mathematical Theory of Communication. *Bell System Tech. J.* 27, 379–423, 623–656. <https://doi.org/10.1002/j.1538-7305.1948.tb01338.x>

Smith, A.B., 2007. Marine diversity through the Phanerozoic, problems and prospects. Bicentennial Review. *J. Geol. Soc.* 1644, 731–745. <https://doi.org/10.1144/0016/76492006-184>

Steeves, R.R., 1981. *A statistical test for significance of peaks in the least squares spectrum*. Collected Papers, Geodetic Survey, Department of Energy, Mines and Resources. Surveys and Mapping Branch, Ottawa Canada, pp. 149–166. <http://www2.unb.ca/gge/Research/GRL/LSSA/Literature/Steeves1981.pdf>

Stefani, F., Xu, M., Sorriso-Valvo, L., Gerbeth, G., Günther, U., 2007. Oscillation or rotation: a comparison of two simple reversal models. *Geophys. Astrophys. Fluid Dyn.* 1013–4, 227–248. <https://doi.org/10.1080/03091920701523311>

Strogatz, S.H., 2000. *Nonlinear Dynamics and Chaos: With Applications to Physics, Biology, Chemistry, and Engineering Studies in Nonlinearity*. CRC Press, United States, 512 pp. ISBN 0738204536

Svensson, I.-M., Bengtsson, A., Bylander, J., Shumeiko, V., Delsing, P., 2018. Period multiplication in a parametrically driven superconducting resonator. *Appl. Phys. Lett.* 113, 022602. <https://doi.org/10.1063/1.5026974>

Tanner L.H., Lucas S.G., 2014. *Limitations of the Astronomically Tuned Timescale: A Case Study from the Newark Basin*. In: Rocha, R., Pais, J., Kullberg, J., Finney, S. (Eds.) *STRATI 2013*, 1st International Congress on Stratigraphy: At the Cutting Edge of Stratigraphy. Springer Geology. https://doi.org/10.1007/978-3-319-04364-7_44

Taylor, J., Hamilton, S., 1972. Some tests of the Vaníček Method of spectral analysis. *Astrophys. Space Sci.* 17, 357–367. <https://doi.org/10.1007/BF00642907>

Uyeda, J.C., Hansen, T.F., Arnold, S.J., Pienaar, J., 2011. The million-year wait for macroevolutionary bursts. *Proc. Natl. Acad. Sci. U.S.A.* 10838, 15908–15913. <https://doi.org/10.1073/pnas.1014503108>

Valet, J.-P., Fournier, A., 2016. Deciphering records of geomagnetic reversals. *Rev. Geophys.* 54, 410–446. <https://doi.org/10.1002/2015RG000506>

Vaníček, P., 1969. Approximate spectral analysis by least-squares fit. *Astrophys. Space Sci.* 44., 387–391. <https://doi.org/10.1007/BF00651344>

Vaníček, P., 1971. Further development and properties of the spectral analysis by least-squares fit. *Astrophys. Space Sci.* 121, 10–33. <https://doi.org/10.1007/BF00656134>

Wells, D.E., Vaníček, P., Pagiatakis, S., 1985. *Least squares spectral analysis revisited*. Department of Geodesy & Geomatics Engineering Technical Report 84, University of New Brunswick, Canada. <http://www2.unb.ca/gge/Pubs/TR84.pdf>

Westerhold, T., Rohl, U., Frederichs, T., Bohaty, S.M., Zachos, J.C., 2015. Astronomical calibration of the geological timescale: closing the middle Eocene gap. *Clim. Past* 119, 1181–1195. <https://doi.org/10.5194/cp-11-1181-2015>

Westerhold, T., Rohl, U., Laskar, J., 2012. Time scale controversy: Accurate orbital calibration of the early Paleogene. *Geochem. Geophys. Geosyst.* 13, Q06015. <https://doi.org/10.1029/2012GC004096>

Wu, H., Zhang, S., Hinnov, L.A., Feng, Q., Jiang, G., Li, H., Yang, T., 2013. Late Permian Milankovitch cycles. *Nat. Commun.* 4, 2452. <https://doi.org/10.1038/ncomms3452>

Yao, N.Y., Nayak, C., Balents, L., Zaletel, M.P., 2020. Classical discrete time crystals. *Nat. Phys.* 16, 438–447. <https://doi.org/10.1038/s41567-019-0782-3>

Yao, N.Y.,—Nayak, C., 2018. Time crystals in periodically driven systems. *Phys. Today* 71, 40–47. <https://doi.org/10.1063/PT.3.4020>